J|A|C|S
ARTICLES
Published on Web 10/23/2003

Homoanomeric Effects in Six-Membered Heterocycles

Igor V. Alabugin,* Mariappan Manoharan, and Tarek A. Zeidan

Contribution from the Department of Chemistry and Biochemistry, Florida State University, Tallahassee, Florida 32306-4390

Received July 15, 2003; E-mail: alabugin@chem.fsu.edu

Abstract: Structural and energetic consequences of homoanomeric n(X) → β-σ*(C−Y) interactions in saturated six-membered heterocycles where X = O, N, S, Se and Y = H, Cl were studied computationally using a combination of density functional theory (B3LYP) and Natural Bond Orbital (NBO) analysis. Unlike the classic anomeric effect where the interacting donor and acceptor orbitals are parallel and overlap sidewise in a π-fashion, orbital interactions responsible for homoanomeric effects can follow different patterns imposed by the geometric restraints of the respective cyclic moieties. For the equatorial β-C−Y bonds in oxa-, thia- and selena-cyclohexanes, only the homoanomeric $n(X)_{ax} \rightarrow \sigma^*(C-Y)_{eq}$ interaction (the Plough effect) with the axial lone pair of X is important, whereas the $n(X)_{eq} \rightarrow \sigma^*(C-Y)_{eq}$ interaction (the W-effect) is negligible. On the other hand, the W-effect is noticeably larger than the $n(X)_{ax} \rightarrow \sigma^*(C-Y)_{eq}$ interaction in azacyclohexanes. Hyperconjugation is a controlling factor which determines relative trends in the equatorial β-C−H bonds in heterocycloxanes. In contrast, all homoanomeric interactions are weak for the respective axial bonds where relative lengths are determined by intramolecular electron transfer through exchange interactions and polarization-induced rehybridization. Although the homoanomeric effects are considerably weaker than the classic vicinal anomeric $n(X)_{ax} \rightarrow \alpha$-$\sigma^*(C-Y)_{ax}$ interactions, their importance increases significantly when the acceptor ability of σ*orbitals increases as a result of bond stretching and/or polarization. Depending on the number of electrons and the topology of interactions, homoconjugation interactions can be cooperative (enhance each other) or anticooperative (compete with each other). Such effects reflect symmetry of the wave function and can be considered as weak manifestations of sigma homoaromaticity or homoantiaromaticity.

Introduction

General rules controlling the interaction of electronic orbitals in space (stereoelectronic effects) are important for understanding molecular properties and chemical reactivity. Although the interaction of π-orbitals, or conjugation, embodied in the most pure form in Hückel theory, has been a prominent feature of theoretical organic chemistry for a long time, the importance of delocalizing interactions involving σ-bonds, or hyperconjugation,[1,2] has not been equally recognized even though Mulliken's pioneering papers on hyperconjugation date back to the early 40s.[3] This is, in a way, surprising because (unlike π-bonds) σ-bonds are present in *every molecule* and, thus, hyperconjugative interactions are ubiquitous in organic chemistry and lead to significant changes in geometry,[4,5] electron density distribution, MO energies, IR-spectra, bond strengths (Bohlmann effect),[6,7] and NMR properties (Perlin effect).[8] In many cases, hyperconjugation influences conformational equilibria,[9−12] modifies reactivity,[13] determines selectivity,[14] and is enhanced dramatically in excited, radical and ionic species.[15] Two-electron/two-orbital hyperconjugative interactions are also proposed to be important components of *inter*molecular interactions, both in ground[16] and transition states.[17,18]

Nonbonding electronic orbitals (lone pairs) are particularly well suited for the role of donor in hyperconjugative interactions and, as a result, stereoelectronic effects involving lone pairs of

(1) Dewar, M. J. S. *Hyperconjugation*; Ronald Press Co.: New York, 1962.
(2) Reed. A. E.; Curtiss, L. A.; Weinhold, F. *Chem. Rev.* **1988**, *88*, 899.
(3) The term "hyperconjugation" was first introduced by Mulliken: Mulliken, R. S. *J. Chem. Phys.* **1939**, *7*, 339. Mulliken, R. S.; Rieke, C. A.; Brown, W. G. *J. Am. Chem. Soc.* **1941**, *63*, 41.
(4) Hyperconjugative interactions in ground state from X-ray geometries: Laube, T.; Ha, T. −K. *J. Am. Chem. Soc.* **1988**, *110*, 5511.
(5) The hyperconjugative effects have to be explicitly used in molecular mechanics parametrization in order to describe properties of covalent bonds accurately. Thomas, H. D.; Chen, K.; Allinger, N. L. *J. Am. Chem. Soc.* **1994**, *116*, 5887.
(6) Bohlmann, F. *Angew. Chem.* **1957**, *69*, 547.
(7) Wolfe, S.; Kim, C. −K. *Can. J. Chem.* **1991**, *69*, 1408.
(8) See refs 16, 19, 22, 23, and 25.
(9) (a) Romers, C.; Altona, C.; Buys, H. R.; Havinga, E. *Top. Stereochem.* **1969**, *4*, 39. (b) Zefirov, N. S.; Schechtman, N. M. *Usp. Khim.* **1971**, *40*, 593. (c) Juaristi, E.; Cuevas, G. *Tetrahedron* **1992**, *48*, 5019. (d) Graczyk, P. P.; Mikolajczyk, M. *Top. Stereochem.* **1994**, *21*, 159.
(10) (a) Kirby, A. J. *The Anomeric Effect and Related Stereoelectronic Effects at Oxygen*; Springer-Verlag: Berlin, 1983. (b) *The Anomeric Effect and Associated Stereoelectronic Effects*; Thatcher, G. R. J., Ed.; ACS Symposium Series 539; American Chemical Society: Washington, DC, 1993. (c) Juaristi, E.; Guevas, G. *The Anomeric Effect*; CRC Press: Boca Raton, FL, 1994. (d) Juaristi, E., Ed., *Conformational Behavior of Six-Membered Rings*: VCH Publishers, New York, 1995. (e) For the most recent experimental example and leading references, see also: Uehara, F.; Sato, M.; Kaneko, C.; Kurihara, H. *J. Org. Chem.* **1999**, *64*, 1436.
(11) (a) Reed, A. E.; Weinhold, F. *Isr. J. Chem.* **1991**, *31*, 277. (b) Goodman, L.; Pophristic, V.; Gu, H. *J. Chem. Phys.* **1999**, *110*, 4268. (c) Goodman, L.; Pophristic, V.; Weinhold, F. *Acc. Chem. Res.* **1999,** *32*, 983. (d) Schreiner, P. R. *Angew. Chem. Int. Ed. Engl.* **2002**, *41*, 3579.
(12) (a) Conformational equilibrium in phosphorus- and silicon-containing systems and hyperconjugation: Cramer, C. J. *J Mol Struct. (Theochem)* **1996**, *370*, 135. (b) Role of lone pairs in internal rotation barriers: Pophristic, V.; Goodman, L.; Guchhait, N. *J. Phys. Chem. A* **1997**, *101*, 4290. (c) Internal rotation barriers in toluenes: Lu, K. T.; Weinhold, F.; Weishaar, J. C. *J. Chem. Phys.* **1995**, *102*, 6787.

10.1021/ja037304g CCC: $25.00

oxygen, nitrogen, sulfur, and other heteroatoms are well documented in the scientific literature. Arguably, the best documented and the most intensively studied of such effects is the anomeric effect.[10,19]

The anomeric effect was originally defined as the preference for an electronegative substituent positioned next to an oxygen atom in a tetrahydropyran ring (or at the anomeric carbon of pyranoses) for occupying an axial rather than an equatorial position.[9,10] It was recognized later that this is a consequence of a more general effect which requires that a lone pair $n(X)$ at heteroatom X and C−Y bond in a YCH_2X moiety are aligned in an antiperiplanar geometry[20−22] that maximizes the hyperconjugative $n(X) \rightarrow \sigma^*(C-Y)$ interaction.[23,24]

In contrast to the classic anomeric effect, *homoanomeric interactions* of heteroatom lone pairs with acceptor orbitals *at the β-carbon atom* are less studied, even though *homoconjugation* is well established in organic chemistry, especially in the chemistry of carbocations.[25] There are numerous indications that topologically similar homoanomeric interactions may exist in six-membered heterocycles with a variety of β-donor groups such as heteroatoms, double bonds (both endo- and exocyclic) and anionic fragments. As a result of such interactions, equatorial substituents in cyclohexanes with π-donating groups at the β-position are expected to display higher reactivity. In line with these expectations, the solvolysis of 3-β-cholesteryl tosylate (or chloride) proceeded 100 times faster than the reaction of the cyclohexyl analogue due to assistance by the β-double bond.[26]

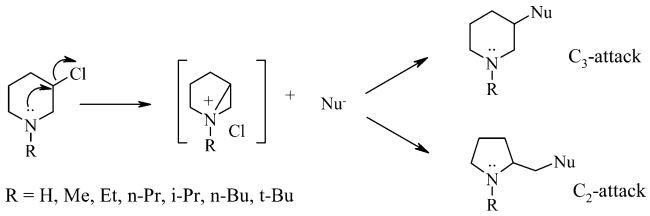

Figure 1. Solvolysis of β-substituted cyclic amines.

In an analogous manner, solvolysis of cyclic amines such as piperidines and pyrrolidines with a leaving group at the β-carbon proceeds through formation of cyclic aziridinium cations due to anchimeric assistance from the nitrogen lone pair (Figure 1).[27] The presence of such intermediates leads to retention of configuration and efficient transfer of chirality in such ring contraction or expansion reactions.[28] This protocol was used for the synthesis of several aza-sugars with promising biological activity.[27] Topologically similar transformations are the key mechanistic steps of Payne and aza-Payne rearrangements.[29]

In addition to the anchimeric assistance in formation of bridged cationic intermediates, there is clear structural and spectroscopic evidence for homoanomeric interactions in neutral ground-state molecules at their energy minimum conformations. For example, the C(5)−H equatorial bond in 1,3-dioxane is longer than the C(5)−H axial bond and the respective direct NMR $^{13}C-^{1}H$ coupling constant is smaller than that for the axial bond ($^1J_{CHeq} < {}^1J_{CHax}$).[54] This phenomenon (the reverse Perlin effect[30]) contrasts with the "normal" situation, e.g., in cyclohexane, where the axial C−H bond is longer and the corresponding $^1J_{CH}$ constant is smaller (the normal Perlin effect).[31] Originally, the reverse Perlin effect in 1,3-dioxane was explained by assuming a homoanomeric $n_{eq} \rightarrow \sigma^*_{eq}$ interaction between the pseudoequatorial lone electron pair on the β-oxygen and the equatorial C(5)−H bond through a W-arrangement of orbitals (the W-effect). A more recent computational study[32] found that the key hyperconjugative interaction leading to the reverse Perlin effect in 1,3-dioxane is that of the equatorial C(5)−H bond with the *pseudoaxial* lone electron pair on the β-oxygen (the Plough effect)[33] and that the W-effect was unimportant in 1,3-dioxane, 1,3-dithiane, and 1,3-oxathiane.[34]

(13) (a) Kinetic α-effect: Baddeley, G. *Tetrahedron Lett.* **1973**, *14*, 1645. Chang, J. −W. A.; Taira, K.; Urano, S.; Gorenstein, D. G. *Tetrahedron* **1987**, *43*, 479. Um, I. H.; Chung, E. K.; Lee, S. M. *Can. J. Chem.* **1998**, *76*, 729. (b) see also, ref 2a. (c) Kinetic anomeric effect: Deslongchamps, P. *Tetrahedron* **1975**, *31*, 2463. Doddi, G.; Ercolani, G.; Mencarelli, P. *J. Org. Chem.* **1992**, *57*, 4431. Roberts, B. P.; Steel, A. J. *Tetrahedron Lett.* **1993**, *34*, 5167. (d) π-Facial diastereoselectivity: Sato, M.; Sunami, S.; Kaneko, C. *Heterocycles* **1995**, *42*, 861, and references sited therein. (e) Photochemical hydrogen abstraction: Wagner, P. J.; Scheve, B. J. *J. Am. Chem. Soc.* **1977**, *99*, 1858. (f) β-Effect of silicon: Lambert, J. B.; Zhao, Y.; Emblidge, R. W.; Salvador, L. A.; Liu, X.; So, J. −H.; Chelius, E. C. *Acc. Chem. Res.* **1999**, *32*, 18. (g) Reactivity of fluoroorganic compounds: Borden, W. T. *J. Chem. Soc., Chem. Commun*. **1998**, 1919. (h) Stereoelectronic effects in the ring-closing metathesis reaction: Maier, M. E. *Angew. Chem., Int. Ed. Engl*. **2000**, *39*, 2073.

(14) Beckwith, A. L. J.; Duggan, P. J. *Tetrahedron* **1998**, *54*, 6919 and the examples cited therein.

(15) (a) Muller, N.; Mulliken, R. S. *J. Am. Chem. Soc.* **1958**, *80*, 3489. Also, see ref 1a. For the recent examples, see: (b) Stability of α-sulfonyl carbanions: Raabe, G.; Gais, H. J.; Fleischhauer. J. *J. Am. Chem. Soc.* **1996**, *118*, 4622. (c) The anomeric effect in 1,3-dioxa systems: Ganguly, B.; Fuchs, B. *J. Org. Chem.* **1997**, *62*, 8892. (c) Kirchen, R. P.; Ranganayakulu, K.; Sorensen, T. S. *J. Am. Chem. Soc.* **1987**, *109*, 7811.

(16) For example, hydrogen bonding: Weinhold, F. *J. Mol. Struct. (Theochem)* **1997**, *398*, 181.

(17) (a) Cieplak, A. S. *J. Am. Chem. Soc.* **1981**, *103*, 4540. (b) Cieplak, A. S.; Tait, B. D.; Johnson, C. R. *J. Am. Chem. Soc*, **1989**, *111*, 8447.

(18) (a) Cherest, M.; Felkin, H.; Prudent, N. *Tetrahedron Lett.* **1968**, *9*, 2199. (b) Cherest, M.; Felkin, H. *Tetrahedron Lett.* **1968**, 2205. (c) Cherest, M. *Tetrahedron* **1980**, *36*, 1593. (d) Ahn, N. T.; Eisenstein, O. *Tetrahedron Lett.* **1976**, *17*, 155. (e) Ahn, N. T. *Top. Curr. Chem.* **1980**, *88*, 145.

(19) (a) Romers, C.; Altona, C.; Buys, H. R.; Havinga, E. *Top. Stereochem.* **1969**, *4*, 39. (b) Zefirov, N. S.; Schechtman, N. M. *Usp. Khim.* **1971**, *40*, 593. (c) Graczyk, P. P.; Mikolajczyk, M. *Top. Stereochem.* **1994**, *21*, 159.

(20) David, S.; Eisenstein, O.; Hehre, W. J.; Salem, L.; Hoffmann, R. *J. Am. Chem. Soc.* **1973**, *95*, 3806.

(21) Wolfe, S. *Acc. Chem. Res.* **1972**, *5*, 102.

(22) The anomeric effect with central atoms other than carbon: Reed, A. E.; Schleyer, P. v. R. *Inorg. Chem.* **1988**, *27*, 3969.

(23) Such requirement is manifested in a plethora of other effects including but not limited to the preference for the staggered conformation of ethane,[11] conformational equilibria of substituted cyclohexanes (Kleinpeter, E.; Taddei, F.; Wacker, P. *Chem. Eur. J.* **2003**, *9*, 1360) preference for the Z-conformation of esters and enhanced reactivity of lactones as well as many other effects on structure and reactivity. For a further discussion and many illustrative examples, see: Kirby, A. J. *Stereoelectronic Effects*; Oxford University Press: New York, 2000.

(24) Although there are several components of the anomeric effect such as an electrostatic component, (e.g., dipole−dipole interactions and steric effects),[9,10] the above hyperconjugative interaction of the antiperiplanar orbitals plays a particularly important role. This is reflected in structural changes (C−Y bond elongation and C−X bond shortening), in distribution of electron density (increased negative charge on Y) and in reactivity (C−Y bond weakening).

(25) Sunko, D. E; Hirsl-Starcevic, S.; Pollack, S. K.; Hehre, W. J. *J. Am. Chem. Soc.* **1979**, *101*, 6163 and references therein. See also the vast literature on nonclassical carbocations.

(26) Winstein, S.; Adams, R. *J. Am. Chem. Soc.* **1948**, *70*, 838.

(27) Fuson, R. C.; Zirkle, C. L. *J. Am. Chem. Soc.* **1948**, *70*, 2760. Reitsema, R. H. *J. Am. Chem. Soc.* **1949**, *71*, 2041. Hammer, C. F.; Heller, S. R.; Craig, J. H. *Tetrahedron* **1972**, *35*, 239 and references therein.

(28) Diastereocontrolled synthesis of enantiopure 5-allylprolinols: Sakagami, H.; Ogasawara, K. *Synlett* **2001**, *1*, 45.

(29) Payne, G. B. *J. Org. Chem.* **1962**, *27*, 3819. Hanson, R. M. *Org. React.* **2002**, *60*, 1. Ibuka, T. *Chem. Soc. Rev.* **1998**, *27*, 145.

(30) The normal Perlin effect in cyclohexane attributed to the obsevation that the axial C−H bonds are longer and weaker than the equatorial bonds as the result of hyperconjugative $\sigma_{C-H} \rightarrow \sigma^*_{C-H}$ interactions with the participation of antiperiplanar C−H bonds.[32] The sensitivity of the direct H−C coupling constants to the subtle structural factors is widely used for stereochemical assignments, especially in carbohydrate chemistry.

(31) Wolfe's new definition of the Perlin effect is given in ref 7.

(32) Alabugin I. V. *J. Org. Chem.*, **2000**, *65*, 3910.

(33) This name was suggested by Professor A. Davies in a private communication. "The Plough" is the British name for the Ursa Major, or "the Big Dipper" constellation.

The question about homoanomeric interactions in other heterocycles is still open. Recently, an elegantly designed experimental study used conformational restraints in 1,3-diazacyclohexanes to fix nitrogen lone pairs in either the axial or equatorial position (vide infra).[35] On the basis of the experimental NMR data, the authors tentatively suggested that a rather weak W-type interaction may operate in 1,5-diazabicyclo-[3.2.1]octanes but could not arrive at a definitive conclusions because of difficulties in unambiguous by assigning the coupling constants and the lack of information about the respective C−H bond lengths. Because a convincing experimental proof[36] for the existence of the W-effect is still unavailable and because homoanomeric interactions in azacyclohexanes were not studied theoretically, we decided to approach this problem computationally. We have placed this analysis in the frame of the general picture of homoanomeric interactions which include the relative role of the W- and the $n_{ax} \rightarrow \sigma^*_{eq}$ homoanomeric effects in aza-, oxa-, thio- and selenaheterocycles. Such a picture is necessary for understanding relative trends in one-bond $^1J_{CH}$ coupling constants, which, in turn, is needed for conformational analysis of carbohydrates, azacarbohydrates, and other substrates of biological interest.[37]

In particular, the present study provides a more detailed account of the homoanomeric interactions in oxa- and thiaheterocycles, expands our computational analysis to N-containing heterocycles and connects theory with the experimental data.[35] After an overview of general factors controlling homoconjugative interactions such as geometric patterns, and properties of donor and acceptor orbitals, we will thoroughly discuss homoanomeric interactions in a variety of saturated heterocycles. We will show that the length of the axial β-C−H bonds is controlled (a) by a previously unknown stereoelectronic effect not associated with hyperconjugative stabilization and (b) by rehybridization of C−H bonds due to the presence of a heteroatom in the ring. After addressing transferability of different stereoelectronic effects between oxa-, thia-, and azacyclohexanes, we will analyze cooperativity/anticooperativity between homoanomeric interactions which can be considered as manifestations of weak σ-homoaromaticity and σ-homoantiaromaticity.

Computational Details and Choice of Method

All structures were fully optimized at the B3LYP[38]/6-31G** level using the GAUSSIAN 98 package.[39] The 6-31G**[40] basis set is commonly used in computational studies on the anomeric effect.[41,50]

Electronic structures of model compounds were studied using Natural Bond Orbital (NBO) analysis.[42] The NBO 4.0[43] program was used to evaluate the energies of hyperconjugative interactions, overlap matrix (S_{ij}) and Fock matrix (F_{ij}) elements[44] corresponding to the orbital interactions, as well as the hybridization and energies of donor and acceptor orbitals. The NBO analysis transforms the canonical delocalized Hartree−Fock (HF) MOs, or corresponding natural orbitals of a correlated description into localized orbitals that are closely tied to chemical bonding concepts. This process involves sequential transformations of nonorthogonal atomic orbitals (AOs) to the sets of "natural" atomic orbitals (NAOs), hybrid orbitals (NHOs), and bond orbitals (NBOs). Each of these localized basis sets is complete and orthonormal. Energies of the corresponding orbitals are the expectation values (diagonal matrix elements) of the Fock or Kohn−Sham operator. Filled NBOs describe the hypothetical strictly localized Lewis structure. The interactions between filled and vacant orbitals represent the deviation of the molecule from the Lewis structure and can be used as a measure of delocalization. This method gives energies of hyperconjugative interactions both by deletion of the off-diagonal Fock matrix elements between the interacting orbitals and from the second-order perturbation approach

(34) The analogous interaction in 1,3-dithianes was even larger in *absolute* magnitude but its *relative* role was less important than in 1,3-dioxane because of the larger magnitude of $\sigma_{C5-Heq} \rightarrow \sigma^*_{C4-S3}$ interactions.
(35) Anderson, J. E.; Cai, J.; Davies, A. G. *J. Chem. Soc., Perkin Trans. 2* **1997**, 2633.
(36) For other interesting structural studies on related systems, see: Reany, O.; Goldberg, I.; Abramson, S.; Golender, L.; Ganguly, B.; Fuchs, B. *J. Org. Chem.* **1998**, *63*, 8850. Ritter, J.; Gleiter, R.; Irngartinger, H.; Oeser, T. *J. Am. Chem. Soc.* **1997**, *119*, 10599.
(37) The representative examples: Church, T. J.; Carmichael, I.; Serianni, A. S. *J. Am. Chem. Soc.* **1997**, *119*, 8946. Tvaroska, I.; Taravel, F. R. *Adv. Carbohyd. Chem.* **1995**, *BI 51*, 15. Peruchena, N. M.; Contreras, R. H. *J. Mol. Struct.* (*Theochem)* **1995**, *338*, 25. Andersson, P.; Nordstrand, K.; Sunnerhagen, M.; Liepinsh, E.; Turovskis, I.; Otting, G. *J. Biomol. NMR.* **1998**, *11*, 445. Callam, C. S.; Gadikota, R. R.; Lowary, T. L. *J. Org. Chem.* **2001**, *66*, 4549. Lewis, B. E.; Schramm, V. L. *Am. Chem. Soc.* **2001**, *123*, 1327. Kamienska-Trela, K.; Wojcik, J. *Nucl. Magn. Reson.* **2001**, *30*, 132.
(38) B3LYP: (a) Becke, A. D. *Phys. Rev. A.* **1988**, *38*, 3098. (b) Lee, C. T.; Yang, W. T.; Parr, R. G. *Phys. Rev. B* **1988**, *37*, 785. (c) Stephens, P. J.; Devlin, F. J.; Chabalowski, C. F.; Frisch, M. J. *J. Phys. Chem.* **1994**, *98*, 11623.
(39) Frisch, M. J.; Trucks, G. W.; Schlegel, H. B.; Scuseria, G. E.; Robb, M. A.; Cheeseman, J. R.; Zakrzewski, V. G.; Montgomery, J. A., Jr.; Stratmann, R. E.; Burant, J. C.; Dapprich, S.; Millam, J. M.; Daniels, A. D.; Kudin, K. N.; Strain, M. C.; Farkas, O.; Tomasi, J.; Barone, V.; Cossi, M.; Cammi, R.; Mennucci, B.; Pomelli, C.; Adamo, C.; Clifford, S.; Ochterski, J.; Petersson, G. A.; Ayala, P. Y.; Cui, Q.; Morokuma, K.; Malick, D. K.; Rabuck, A. D.; Raghavachari, K.; Foresman, J. B.; Cioslowski, J.; Ortiz, J. V.; Stefanov, B. B.; Liu, G.; Liashenko, A.; Piskorz, P.; Komaromi, I.; Gomperts, R.; Martin, R. L.; Fox, D. J.; Keith, T.; Al-Laham, M. A.; Peng, C. Y.; Nanayakkara, A.; Gonzalez, C.; Challacombe, M.; Gill, P. M. W.; Johnson, B. G.; Chen, W.; Wong, M. W.; Andres, J. L.; Head-Gordon, M.; Replogle, E. S.; Pople, J. A. *Gaussian 98*, revision A.9; Gaussian, Inc.: Pittsburgh, PA, 1998.
(40) Francl, M. M.; Pietro, W. J.; Hehre, W. J.; Binkley, J. S.; Gordon, M. S.; Defrees, D. J.; Pople, J. A. *J. Chem. Phys.* **1982**, *77*, 3654.
(41) Carballeira, L.; Perez-Juste, I. *J. Org. Chem.* **1997**, *62*, 6144.
(42) For an illustrative rather than an exhaustive list of recent applications of NBO method for analysis of chemical bonding see: Reed, A. E.; Weinhold, F. *Isr. J. Chem.* **1991**, *31*, 277. Goodman, L.; Pophristic, V. T. *Nature* **2001**, *411*, 565. Salzner, U.; Schleyer P. v. R. *J. Org. Chem.* **1994**, *59*, 2138. Gleiter, R.; Lange, H.; Borzyk, O. *J. Am. Chem. Soc.* **1996**, *118*, 4889. Klod, S.; Koch, A.; Kleinpeter, E. *J. Chem. Soc., Perkin Trans. 2* **2002**, 1506. Wilkens, S. J.; Westler, W. M.; Weinhold, F.; Markley, J. L. *J. Am. Chem. Soc.* **2002**, *124*, 1190. van der Veken, B. J.; Herrebout, W. A.; Szostak, R.; Shchepkin, D. N.; Havlas, Z.; Hobza, P. *J. Am. Chem. Soc.* **2001**, *123*, 12 290. Cortes, F.; Tenorio, J.; Collera, O.; Cuevas, G. *J. Org. Chem.* **2001**, *66*, 2918. Sadlej-Sosnowska, N. *J. Org. Chem.* **2001**, *66*, 8737. Uddin, J.; Boehme, C.; Frenking, G. *Organometallics* **2000**, *19*, 571. Gilbert, T. M. *Organometallics* **2000**, *19*, 1160. Munoz, J.; Sponer, J.; Hobza, P.; Orozco, M.; Luque, F. J. *J. Phys. Chem. B.* **2001**, *105*, 6051 Xie, Y.; Grev, R. S.; Gu, J.; Schaefer, H. F., III; Schleyer, P. v. R.; Su, J.; Li, X.-W.; Robinson, G. H. *J. Am. Chem. Soc.* **1998**, *120*, 3773. Paddon-Row, M. N.; Shephard, M. J. *J. Am. Chem. Soc.* **1997**, *119*, 5355.
(43) NBO 4.0. Glendening, E. D.; Badenhoop, J. K.; Reed, A. E.; Carpenter, J. E.; Weinhold, F. Theoretical Chemistry Institute, University of Wisconsin, Madison, WI, 1996.
(44) Fock matrix (F_{ij}) elements correspond to the familiar resonance integrals in simple MO theory. It describes electronic interaction between two orbitals *i* and *j*.
(45) Reed, A. E.; Curtiss, L. A.; Weinhold, F. *Chem. Rev.* **1988**, *88*, 899.
(46) Previously, we showed that the hyperconjugative energies estimated by second-order perturbation and deletion approaches are in an excellent agreement with each other.[59]
(47) (a) Weinhold F. In Schleyer P.v.R., Ed. *Encyclopedia of Computational Chemistry*; Wiley: New York **1998**, *3*, 1792. (b) See also: www.chem-.wisc.edu/~nbo5.
(48) Reed, A. E.; Weinhold, F. *J. Chem. Phys.* **1985**, *83*, 1736.
(49) (a) Danishefsky, S. J.; Langer, M. *Org. Chem.* **1985**, *50*, 3672. (b) Vedejs, E.; Dent, W. H. *J. Am. Chem. Soc.* **1989**, *111*, 6861. (c) Vedejs, E.; Dent, W. H.; Kendall, J. T.; Oliver, P. A. *J. Am. Chem. Soc.* **1996**, *118*, 3556. (d) Cohen, T.; Lin, M. -T. *J. Am. Chem. Soc.* **1984**, *106*, 1130. (e) Rychnovsky, S. D.; Mickus D. E. *Tetrahedron Lett.* **1989**, *30*, 3011.
(50) Salzner, U.; Schleyer P. v. R.*J. Org. Chem.* **1994**, *59*, 2138.
(51) Cuevas, G.; Juaristi, E.; Vela, A. *J. Mol. Struct. (Theochem)* **1997**, *418*, 231.
(52) Juaristi, E.; Cuevas, G.; Vela, A. *J. Am. Chem. Soc.* **1994**, *116*, 5796. Juaristi, E.; Rosquete-Pina, G. A.; Vazquez-Hernandez, M.; Mota, A. J. *Pure App. Chem.* **2003**, *75*, 589.
(53) Freeman, F.; Le'Kelly T. *J. Phys. Chem. A.* **2003**, *107*, 2908. Freeman, F.; Do' Katie U. *J. Mol. Struc. (Theochem)* **2002**, *577*, 43.
(54) (a) Anderson, J. E.; Bloodworth, A. J.; Cai, J. Q.; Davies, A. G.; Tallant, N. A. *J. Chem. Soc., Chem. Commun.* **1992**, 1689. (b) Anderson, J. E.; Bloodworth, A. J.; Cai, J. Q.; Davies, A. G.; Schiesser C. H. *J. Chem. Soc. Perkin Trans. 2* **1993**, 601. (c) Cai, J. Q.; Davies, A. G.; Schiesser, C. H. *J. Chem. Soc., Perkin Trans. 2* **1994**, 1151. (d) see also ref 35.

$$E(2) = -n_\sigma \frac{<\sigma/F/\sigma^*>^2}{\epsilon_{\sigma^*} - \epsilon_\sigma} = -n_\sigma \frac{F_{ij}^{\ 2}}{\Delta E} \quad (1)$$

where $<\sigma/F/\sigma^*>$, or F_{ij} is the Fock matrix element between the *i* and *j* NBO orbitals, ϵ_s and ϵ_{σ^*} are the energies of σ and σ^* NBOs, and σ_s is the population of the donor s orbital.[45,46] Detailed descriptions of the NBO calculations are available in the literature.[45,47,48]

Results and Discussion

Choice of Model Substrates. Rigid geometries of six-membered heterocycles such as tetrahydropyran, thiacyclohexane and piperidine lend themselves to investigation of stereoelectronic effects.[10,49] This choice of heteroatoms allowed us to scan a variety of donor lone pairs of different hybridizations, energies, spatial orientations, and sizes—the factors which are crucial for stereoelectronic interactions. To understand the cooperativity of homonoanomeric effects, we have extended our analysis to 1,3-diheterocyclohexanes which were also a subject of several recent theoretical[7,50−53] and experimental[52,54−58] studies. Finally, cyclohexane was used as a useful reference point.

All model compounds with their respective equatorial and axial C−H bond lengths at the β-carbons are listed in Figure 2. Interestingly, depending on the nature of X, either elongation or shortening is observed for the equatorial C−H bonds but bond shortening was found for the axial C−H bonds compared with the respective C−H bond lengths in cyclohexane. We will discuss the origin of these structural effects in detail later after a general overview of homoanomeric interactions. We will start with the description of four main geometries for homoanomeric interactions followed by an analysis of general factors which control the relative magnitudes of these effects.

General Considerations

On a very basic level, the magnitude of the stabilization produced by a two-electron/two-orbital hyperconjugative interaction depends on four factors: (a) the acceptor ability of the empty orbital,[59] (b) the donor ability of the filled orbital,[60] as well as (c) the energy gap, and (d) the spatial overlap between the donor and acceptor orbitals which is determined by molecular geometry.

Four Main Geometries for Homoanomeric Interactions. Two main mechanisms which transfer the effect of heteroatoms to β-C−H bonds are the vicinal σ(C−X) → σ^*(C−H)$_{eq}$ and σ(C−H)$_{eq}$ → σ^*(C−X) interactions discussed in detail in earlier work[32] and the direct n(X) → σ^*(C−H) homoanomeric interactions which are the subject of this paper. The possible geometries for the homoanomeric interactions are summarized in Figure 3 and Figure 4.

A. Interactions Involving the Equatorial C−Y Bonds: The W-Effect and $n(X)_{ax} \rightarrow \sigma^*(C-Y)_{eq}$ (Plough) Interaction. The conceptual difference between the two homoanomeric effects involving the equatorial C−H (or C−Y) bonds in heterocyclohexanes is illustrated in Figure 3, whereas the energies and other important parameters of the corresponding interactions are summarized in Figure 4. According to the computational data in Figure 4, the W-interaction is stronger than the $n_{ax} \rightarrow \sigma^*_{eq}$ interaction in the case of nitrogen but not in the cases of oxygen, sulfur, and selenium. This may seem surprising because the geometry for the W-interaction looks intrinsically better in all of the model heterocycles. However, the favorable directionality of the equatorial lone pairs in O-, S-, and Se− heterocycles is counterbalanced by their unfavorable hybridization (vide infra). The larger orbital lobe of the equatorial lone pairs is directed away from the σ^*(C−H or C−X) orbital, and the latter has to interact with the smaller back lobe of the lone pair. The size of the back lobe which is responsible for the homoanomeric interactions increases with the percentage of p-character in the lone pair: it is larger for the ca. sp^5 lone pair of nitrogen and much smaller for the $sp^{0.4}$ lone pair of sulfur.

B. Interactions Involving the Axial C−H Bonds. To the best of our knowledge, the two homoanomeric interaction patterns which involve the axial C−H bonds—the $n_{eq} \rightarrow \sigma^*_{ax}$ interaction (c) and the U-type $n_{ax} \rightarrow \sigma^*_{ax}$ interaction (d) (Figure 3) have not been analyzed before. This is not surprising, because for relatively weak acceptors, e.g., the σ^*(C−H) orbitals, these interactions are small. Note, however, that in S-heterocycles *both* interactions (c) and (d) are still stronger than the extensively discussed W-effect (a) (see Figure 4).

The relative magnitudes of these effects are controlled by the topology of orbital interactions. For example, the $n_{eq} \rightarrow \sigma^*_{ax}$ interaction seems, at first glance, to be similar in geometry to the rather favorable $n_{ax} \rightarrow \sigma^*_{eq}$ interaction with the only difference being the donor orbital is aimed at the center (rather than at the end) of the acceptor orbital. However, the magnitude of this interaction is only 1/6th of the $n_{ax} \rightarrow \sigma^*_{eq}$ interaction in O-heterocycles and this effect is essentially absent in N-heterocycles. This finding is not surprising because, although this interaction is favored by geometry, it is disfavored by orbital symmetry (similar to the front attack in S_N2 reactions)—the donor orbital is aimed at a node at the center of the σ^* orbital (Figure 4).

Finally, the rather weak $n(X)_{ax} \rightarrow \beta$-$\sigma^*(C-H)_{ax}$ interaction is interesting because it is closest to the sidewise π-type pattern of the classic anomeric effect. Although this interaction is essentially zero in tetrahydropyrane (X = O), it becomes noticeable when the size of lone pairs increases (X=S, Se) or when hybridization effects make the orientation and size of the front lobe more favorable for the interaction (X = N).

Although the magnitude of homoanomeric interactions depends on the rather complex interplay of geometric factors and intrinsic properties of interacting orbitals, the relative trends in the energies of homoanomeric interactions are readily explained by differences in the overlap and Fock matrix elements (S_{ij} and F_{ij}[44] elements) corresponding to these interactions. According to eq 1, the energy of a hyperconjugative interaction is directly proportional to the square of the respective F_{ij} element, and the correlation between these two quantities is excellent (R^2 >

(55) (a) Anet, F. A.L.; Kopelevich, M. *J. Am. Chem. Soc.* **1986**, *108*, 2109. b) Anet, F. A. L.; Kopelevich, M. *J. Chem. Soc., Chem. Comm.* **1987**, 595.
(56) (a) Juaristi, E.; Cuevas, G. *Tetrahedron Lett.* **1992**, *33*, 1847. (b) Juaristi, E.; Cuevas, G.; Flores-Vela, A. *Tetrahedron Lett.* **1992**, *33*, 6927.
(57) Bailey, W. F.; Rivera, A. D.; Rossi, K. *Tetrahedron Lett.* **1988**, *29*, 5621.
(58) Terec, A.; Grosu, I.; Ple, G.; Muntean, L.; Mager, S. *Heterocycles* **2003**, *60*, 1477.
(59) Alabugin I. V.; Zeidan, T. A. *J. Am. Chem. Soc.* **2002**, *124*, 3175.
(60) Donor ability of σ C−X bonds where X is the first row element from Li to F: Apeilog, Y.; Schleyer, P. v. R.; Pople, J. A. *J. Am. Chem. Soc.* **1977**, *99*, 5901. For a recent study with a particularly interesting discussion of donor ability of C−C and C−H bonds see also: Rablen, P. R.; Hoffmann, R. W.; Hrovat, D. A.; Borden, W. T. *J. Chem. Soc., Perkin Trans. 2* **1999**, 1719.

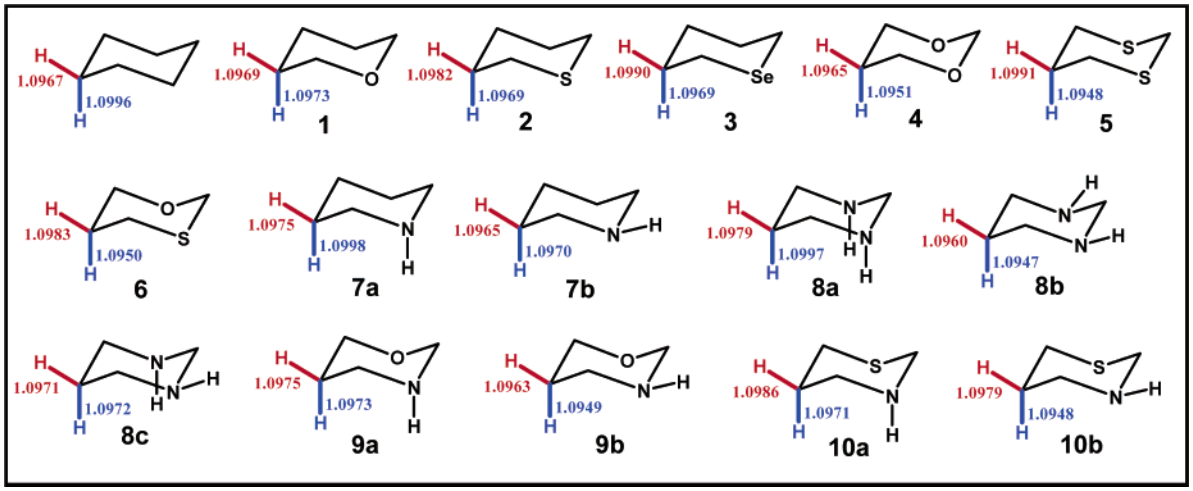

Figure 2. C−H bond lengths at the β-carbons in the model six-membered saturated heterocycles (and cyclohexane) obtained by B3LYP/6-31G** calculations.

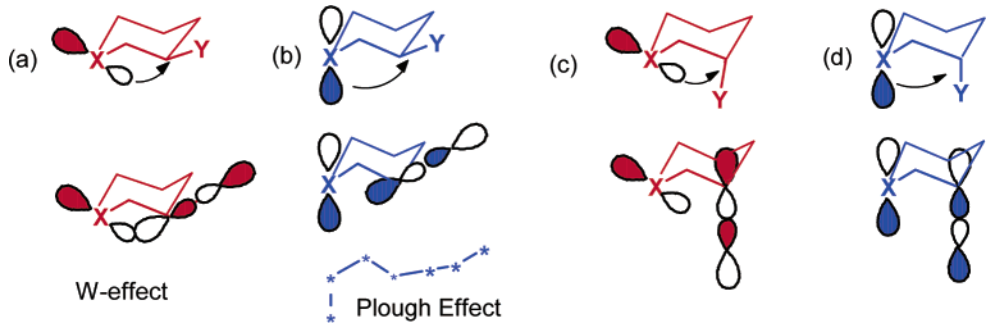

Figure 3. Schematic representation of four possible homoanomeric interactions (a−d) in six-membered saturated heterocycles. At this point, differences in hybridization are neglected. See Figure 4 for a more detailed analysis.

0.99).[61] The analogous correlation with the overlap integral is less reliable and should be used only in a qualitative sense (see the Supporting Information section for these plots).

Properties of Donor Orbitals

Hybridization of Lone Pairs. In this section, we discuss hybridizations, shapes, and energies of donor orbitals for the most important cases (X = O, S, Se, N) (Table 1 and Figure 5). Differences in hybridization are particularly important for stereoelectronic interactions due to several reasons. First, hybridization is directly related to molecular geometry and determines the direction in which nonbonding orbitals are projected in space (the valence angles). Such differences in projection trajectory can have significant consequences for the overlap with acceptor orbitals. Second, hybridization controls the relative size of the two lobes of a lone pair. The front and back lobes are equivalent for purely p-lone pairs whereas the back lobe decreases in size with decrease in the p-character in hybrid sp^n lone pairs. Third, hybridization of a donor orbital is related to its absolute energy (Figure 5). Increase in the p-character leads to increase in orbital energy which decreases the energy gap between the donor lone pair and an acceptor σ^*- or π^*-orbital. In general, donor ability decreases with an increase in the s-character of a lone pair and lone pairs with 100% p-character are intrinsically better donors than respective sp^n hybrids.

A. Oxygen. There are two alternative descriptions of hybridization of the two oxygen lone pairs in the literature. In the first description, both oxygen lone pairs are considered identical and sp^3-hybridized. In the second description, hybridization of the two lone pairs is different—one of them is a sp-hybrid, whereas the other is a pure p-orbital. For some purposes these two descriptions are identical (mixing of a sp- and a p-orbital gives two sp^3 hybrid orbitals). However, these two models become nonequivalent in the presence of intramolecular orbital interactions where the symmetry of interaction, or the energy of the nonbonding electrons, is crucial. In such cases, it is generally considered necessary to use the second representation.[2] This representation is more consistent with data from photoelectron spectroscopy and with the general principle that hybridization is a dynamic property aimed at maximizing chemical bonding.[62] For example, in tetrahydropyran, the presence of a higher energy p-orbital (instead of an sp^3 hybrid) parallel to the vicinal axial acceptors maximizes the hyperconjugative anomeric $n \rightarrow \sigma^*$(C−H/C−Y) interaction. NBO analysis which determines "the best hybrids" describing a Lewis structure finds two lone pairs of different hybridization in tetrahydropyran: a purely p-orbital and a $sp^{1.3}$ hybrid. The deviation from sp hybridization predicted by the idealized model is readily explained by Bent's rule.[63,64] According to this rule, atoms tend to maximize the amount of s-character in hybrid orbitals aimed toward electropositive substituents and tend to

(61) Obviously, such high quality of this correlation is observed in this case only because the energy gap between the donor and acceptor orbitals (the ΔE term) is quite close in these molecules.

(62) For consequences of this notion for the "improper" or "blue-shifted" hydrogen bonding see: Alabugin, I. V.; Manoharan, M.; Peabody S.; Weinhold, F. *J. Am. Chem. Soc.* **2003**, *125*, 5973.

(63) Bent, H. A. *Chem. Rev.* **1961**, *61*, 275.

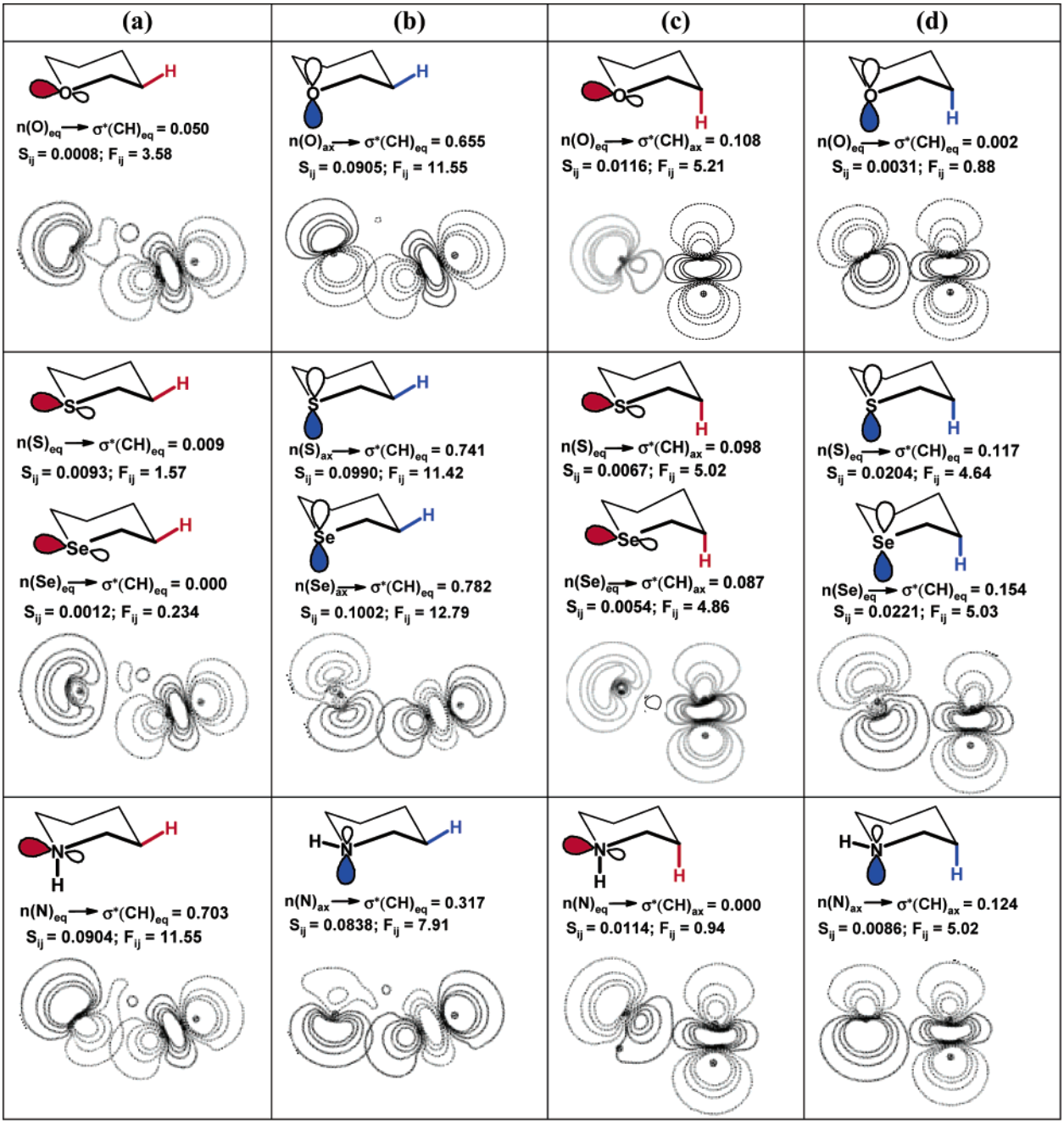

Figure 4. NBO plots of various homoanomeric interactions in selected saturated heterocycles (X = N, O, S) along with the deletion energies (kcal mol^{-1}), overlap matrix elements, S_{ij} (a.u.) and Fock matrix elements, F_{ij} (kcal mol^{-1}) for the corresponding interactions (X = N, O, S, Se). In every case, the orbitals were sliced by the HCX plane where H is either an axial or an equatorial β-hydrogen atom and where heteroatom X = N, O, S. The HCX planes for equatorial and axial hydrogens are not identical which leads to the slightly different shapes of some of the lone pairs.

direct hybrid orbitals with the larger amount of p-character toward more electronegative substituents. Because carbon is less electronegative than oxygen, hybridization of the oxygen orbital in the C−O bonds is sp$^{2.6}$ instead of the idealized sp^3 hybridization. In other words, the increased s-character of the oxygen hybrid orbitals in O−C bonds leaves more p-character for the oxygen lone pairs.

B. Sulfur and Selenium. In contrast to oxygen, the sulfur atom in thiacyclohexane uses *more* p-character (sp$^{5.55}$) in its bond with carbon than one would expect from the idealized model. As a result, only a little p-character is left for the equatorial lone pair (sp$^{0.4}$). This makes this lone pair a relatively poor donor and explains the origin of the drastic differences between the equatorial lone pairs of sulfur and oxygen in Table 1. The change in hybridization also unfavorably influences the shape of the equatorial sulfur lone pair and decreases the relative

(64) For selected applications of Bent's rule see: Baldridge, K. K.; Siegel, J. S. *Chem. Rev.* **2002**, *124*, 5514. Lemke, F. R.; Galat, K. J. Youngs, W. J. *Organometallics* **1999**, *18*, 1419. Kaupp, M.; Malkina, O. L. *J. Chem. Phys.* **1999,** *108*, 3648. Palmer, M. H. *J. Mol. Struct.* **1997**, *405*, 179. Palmer, M. H. *J. Mol. Struct.* **1997**, *405*, 193. Jonas, V.; Boehme, C.; Frenking G. *Inorg. Chem.* **1996**, *35*, 2097. Root, D. M.; Landis, C. R.; Cleveland, T. *J. Am. Chem. Soc.* **1993**, *115*, 4201. Kaupp, M.; Schleyer, P. v. R. *J. Am. Chem. Soc.* **1993**, *115*, 1061. Fantucci, P.; Valenti, V. *J. Chem. Soc., Dalton Trans.* **1992**, 1981. Xie, Y. M.; Schaefer, H. F.; Thrasher, J. S. *J. Mol. Struct. (Theochem)* **1991**, *80*, 247. For the limitations of Bent's rule in treating organometallic compounds see: Kaupp, M. *Chem. Eur. J.* **1999**, *5*, 3631.

Table 1. NBO s-character, Hybridization, and Energy of All Lone Pairs (X = N, O, S, Se) in Heterocycles 1−3,7 Calculated at the B3LYP/6-31G** Level (B3LYP/6-311++G** values are in *italics*), the NBO Plots of the Lone Pairs and s-Character in C−X Bonds

	s-character in n(X), %[a]	sp^n(X)	E(X), a.u.[a]	$n(X)_{ax}$,[c]	$n(X)_{eq}$,[c]	s-character in C-X, %[b]
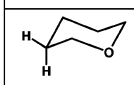	0.03 (44.16) *0.04(43.47)*	p($sp^{1.26}$) *p($sp^{1.30}$)*	-0.27(-0.54) *-0.29(-0.55)*	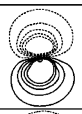	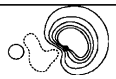	20.53 (C); 27.89 (O) *20.97 (C); 28.31 (O)*
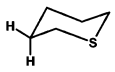	0.03(69.89) *0.00(69.80)*	p ($sp^{0.43}$) *p($sp^{0.44}$)*	-0.22(-0.61) *-0.23(-0.62)*			20.54 (C); 15.18 (S) *20.93 (C); 15.27 (S)*
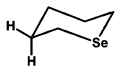	0.05 (76.66) *0.03 (77.13)*	p($sp^{0.30}$) *p($sp^{0.30}$)*	-0.21(-0.67) *-0.21(-0.70)*	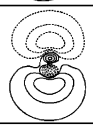	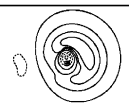	18.51 (C); 11.74 (Se) *19.43 (C); 11.55 (Se)*
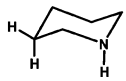	17.99 *16.16*	$sp^{4.55}$ *$sp^{5.18}$*	-0.27 *-0.28*	-	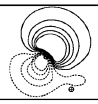	23.51 (C); 29.94 (N) *24.24 (C); 31.07 (N)*
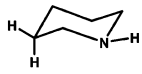	17.86 *16.99*	$sp^{4.59}$ *$sp^{4.88}$*	-0.27 *-0.28*		-	23.62 (C); 29.65 (N) *24.30 (C); 30.50 (N)*

[a]For X=O, S, Se, the data for the equatorial lone pairs are given in parentheses. [b]s-Character in hybrid orbitals forming C−X (X = N, O, S, Se) bonds. [c] The axial and equatorial lone pairs are drawn as dissected by H_{ax}−C3−X1 or H_{eq}−C3−X1 planes, respectively.

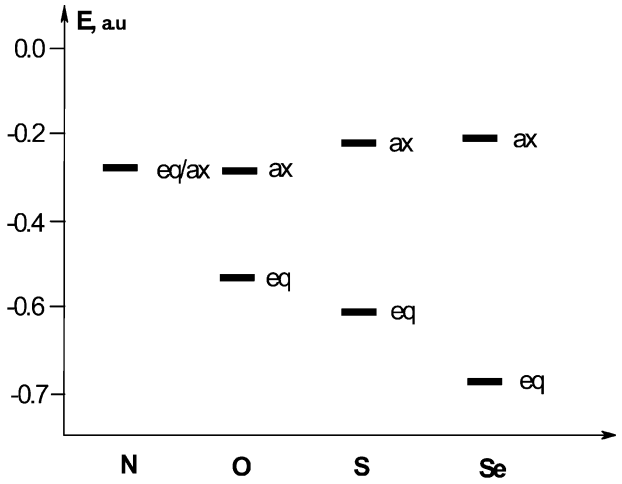

Figure 5. NBO energies (in a.u., 1 au = 627.5 kcal/mol) of axial and equatorial lone pairs in oxa-, thia-, selena-, and azacyclohexane calculated at the B3LYP/6-31G** level.

size of the back lobe responsible for overlap with the acceptor σ^* orbital. These trends are further enhanced for Se.

In contrast to the equatorial lone pairs, the axial lone pairs of S and Se have 100% p-character and, except for the internal nodal structure, are similar in properties to the respective O lone pair. In particular, their donor ability toward β−CH antibonding orbitals is comparable with and even larger than that of oxygen p-lone pairs and increases in the order of O < S < Se. This order of donor ability is unusual and opposite to that observed in anomeric $n(X) \rightarrow \alpha\text{-}\sigma^*(C-H)_{ax}$ interactions: O > S > Se (see Table S1 in the Supporting Information). Interestingly, donation to a stronger acceptor such as σ^*(C−Cl) orbitals in homoanomeric interactions also follows the O > S > Se order. These differences in the trends involving the C−H and C−Cl bonds as acceptors can be rationalized qualitatively using the differences in hardness and softness of the donor/acceptor pair or quantitavely through NBO dissection of the interaction energies given in eq 1. According to NBO analysis, the relative trends in the donor abilities of the chalcogen lone pairs toward σ^*(C−H) orbitals are controlled by decreasing the ΔE term (the energy gap) in eq 1 (see Table S2 in the Supporting Information), whereas the opposite relative trends in the donor abilities toward σ^*(C−Cl) orbitals are explained by larger changes in the F_{ij} term (electronic coupling between the donor and acceptor orbitals).

C. Nitrogen. Nitrogen is more electronegative than carbon and hydrogen and, as expected from Bent's rule, it uses hybrid orbitals with increased s-character for formation of N−C and N−H bonds (Table 1). This leaves more p-character for the lone pairs compared to what one would expect from the textbook sp^3 hybridization picture. This phenomenon leads to the well-known deviation of valence angles at nitrogen from the classic tetrahedral angle and contributes to the relatively high donor ability of nitrogen lone pairs.

Because hybridization of the nitrogen lone pair is directly tied to the degree of pyramidalization and valence angles at nitrogen, it is also sensitive to perturbation in molecular structure and to the level of theory used for the computations (Table 1).

The effects of N-substitution on hybridization and properties of nitrogen lone pairs are further analyzed in Table 2. In general, an increase in the size of alkyl substituents at nitrogen leads to an increase in p-character of the nitrogen lone pairs. This increase is larger when the substituent is axial where it is likely to be associated with the changes in geometry (flattening at the nitrogen atom) needed to alleviate 1,3-diaxial steric interactions. This notion is consistent with the especially large effect of the *tert*-Bu group. Note, however, that the magnitude of the $n(N) \rightarrow \sigma^*(C-Cl)_{eq}$ interaction is changed only slightly in response to these changes in hybridization.[65] Note also that the W-interaction is more than two times larger than the $n(N)_{ax} \rightarrow \sigma^*(C-Cl)_{eq}$ interaction.

(65) For an interesting example of the varying rates of solvolysis of N-substituted 3-Cl−N-alkyl-piperidines, see: Hammer, C. F.; Heller, S. R.; Craig, J. H. *Tetrahedron* **1972**, *35*, 239.

Table 2. Relative Energies (kcal mol^{-1}) of Two Conformers of 3-Cl−N-alkyl-Piperidines, Energies of Homoanomeric Interactions in ($n \rightarrow \sigma^*$) i.e., between the Axial and Equatorial Lone Pairs of N and Equatorial β(C−Cl)$_{eq}$ Bond (kcal mol^{-1}), Charge on Cl Atom (e), Populations of Lone Pair in X (e), as well as in $\sigma^*(\beta C-Cl)_{eq}$, Distance of $\beta C-Cl_{Eq}$ Bond (Å) and the s-Character of N (%) Computed at the B3LYP/6-31G** Level Using NBO Procedure

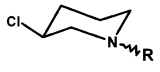	ΔE (eq/ax)	C-Cl$_{eq}$	E[n(N)→ σ*(CCl$_{eq}$)]	*q(Cl)*	pop n (N)	s-char of N	pop σ(CCl$_{eq}$)	pop σ* (CCl$_{eq}$)
R = H$_{eq}$ (**15a**)	0.1	1.8309	0.73	-0.098	1.919	17.27	1.986	0.0354
R = H$_{ax}$ (**15b**)	0.0	1.8352	1.55	-0.102	1.911	16.90	1.986	0.0443
R = Me$_{eq}$ (**16a**)	0.0	1.8303	0.59	-0.095	1.878	14.98	1.986	0.0346
R = Me$_{ax}$ (**16b**)	2.7	1.8337	1.41	-0.099	1.873	12.48	1.985	0.0403
R = Et$_{eq}$ (**17a**)	0.0	1.8311	0.59	-0.096	1.881	14.93	1.986	0.0351
R = Et$_{ax}$ (**17b**)	2.4	1.8347	1.42	-0.102	1.874	12.01	1.985	0.0417
R = *n*-Pr$_{eq}$ (**18a**)	0.0	1.8313	0.61	-0.097	1.881	14.76	1.986	0.0351
R = *n*-Pr$_{ax}$ (**18b**)	2.3	1.8349	1.43	-0.102	1.874	11.61	1.985	0.0420
R = *i*-Pr$_{eq}$ (**19a**)	0.0	1.8324	0.54	-0.098	1.883	15.07	1.985	0.0355
R = *i*-Pr$_{ax}$ (**19b**)	2.0	1.8360	1.45	-0.104	1.874	11.68	1.985	0.0423
R = *n*-Bu$_{eq}$ (**20a**)	0.0	1.8314	0.61	-0.097	1.881	14.80	1.986	0.0352
R = *n*-Bu$_{ax}$ (**20b**)	2.3	1.8346	1.43	-0.102	1.874	11.70	1.985	0.0419
R = *t*-Bu$_{eq}$ (**21a**)	0.0	1.8336	0.86	-0.101	1.881	12.81	1.986	0.0371
R = *t*-Bu$_{ax}$ (**21b**)	3.7	1.8378	1.62	-0.108	1.857	5.54	1.985	0.0444

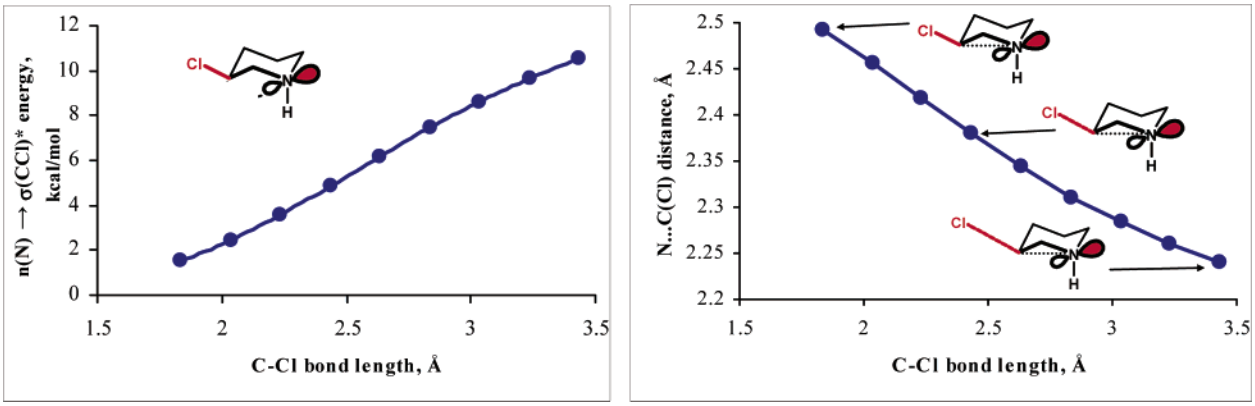

Figure 6. Correlations of C−Cl distance with energy of n(N) → σ^*(C−Cl) interaction and with the N···C(Cl) distance during the process of C−Cl bond stretching in 3-chloropiperidine.

Energies of Lone Pairs. The interaction energy is inversely proportional to the energy gap, ΔE in eq 1, which is determined by the relative energies of lone pairs and antibonding orbitals. Relative trends in the orbital energies can be readily understood in terms of their hybridization (percentage of s-character) and electronegativity of X. Increase in electronegativity and decrease in p-character lower the orbital energies of lone pairs (Figure 5). Interestingly, although oxygen is more electronegative than nitrogen, the purely p axial[66] lone pair on oxygen has essentially the same energy as the ca. sp^5 axial and equatorial nitrogen lone pairs. In this case, effects of hybridization and electronegativity compensate each other. Another interesting trend is observed for the lone pairs of chalcogens: the energies (and donor ability) of axial lone pairs increase when going from oxygen to selenium (O < S < Se), whereas the energies and donor ability of equatorial lone pairs follow the opposite direction (O > S > Se). The first trend is explained by the difference in electronegativity and the period number, the second trend by the increase in the s-character for S and Se relative to that of O. As a result of these two effects, the energy gap between the axial and equatorial lone pairs of chalcogens increases with their atomic number. In every case, the higher energy axial orbitals with 100% p-character should be intrinsically better donors than the respective equatorial sp^n hybrids.

An important conclusion from the above analysis is that O- and S-heterocycles are considerably different from their N-analogues and, thus, stereoelectronic effects observed in O-heterocycles cannot be automatically transferred to the N-heterocycles and vice versa. The analogy between different chalcogens (O, S, Se) is generally more reliable but the differences in the magnitudes of $n_{ax} \rightarrow \sigma^*_{ax}$ interactions call for caution as well.

Properties of Acceptor Orbitals

Effects of Polarization of Acceptor Bonds. In this section, we will show how even small homoanomeric effects can be dramatically enhanced in the presence of stronger acceptor orbitals. Relative trends in the acceptor ability of σ-bonds have been described in the recent literature and the C−Cl bond is known to be among the strongest σ-acceptors.[59] Therefore, it is not surprising that the magnitude of generally small homoanomeric interactions discussed above (less than 1 kcal/mol)

(66) Because hybridization of two lone pairs on oxygen and other chalcogens is different from hybridization of axial and equatorial C−H bonds in cyclohexane, the valence angles between the two lone pairs differ to some extent from those characteristic for the classic axial and equatorial ligands. It is more correct to call these lone pairs pseudoaxial and pseudoequatorial but because it is rarely done so, we will continue using the words "axial" and "equatorial" to distinguish between the two types of lone pairs in this paper.

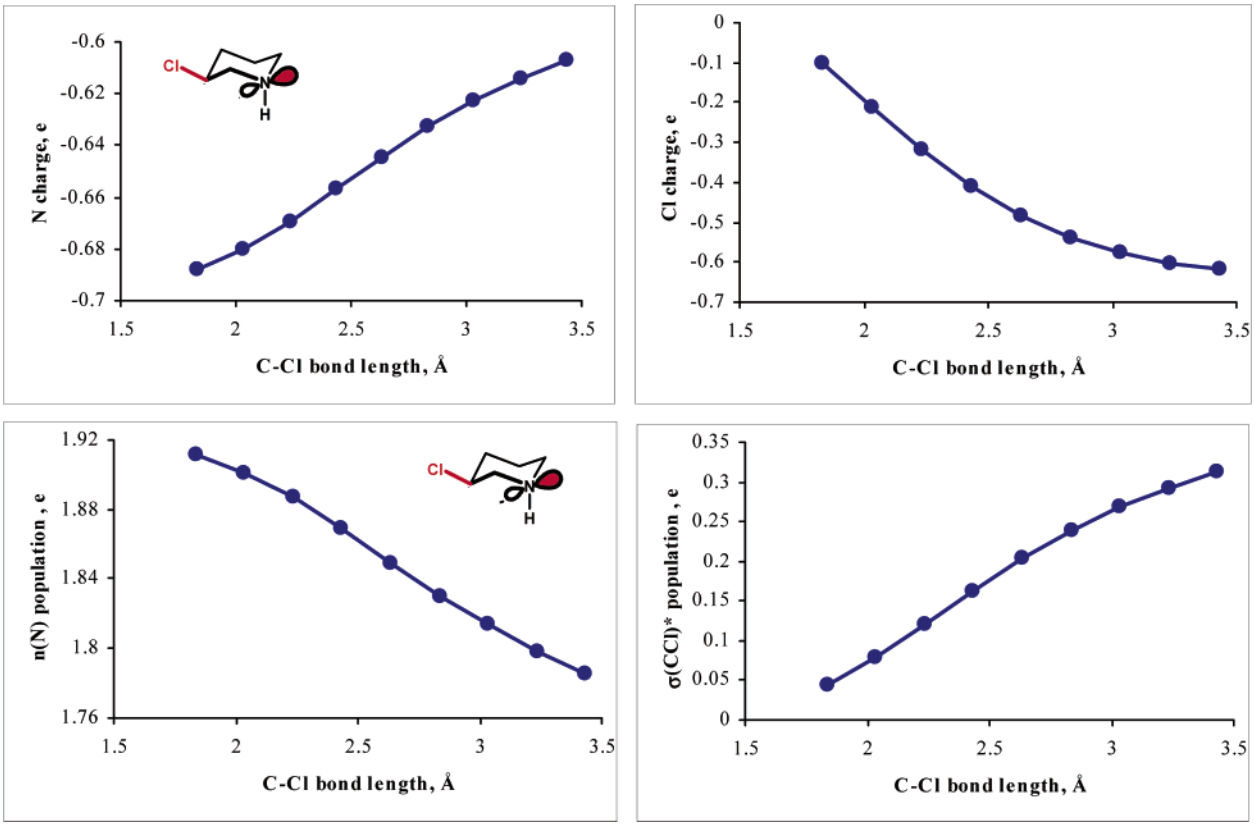

Figure 7. Correlations of C−Cl distance with the natural (NBO) charges at N and Cl, and with populations of nitrogen lone pair and σ^*(C−Cl) orbital (in electrons) during the process of C−Cl bond stretching in 3-chloropiperidine calculated at the B3LYP/6-31G** level.

increases dramatically (more than 2-fold) in the case of a stronger acceptor such as a σ^*(C−Cl) orbital (Table 3). Importantly, despite the difference in absolute magnitude all homoanomeric interactions and structural effects discussed for β-C−H bonds are present for the β-C−Cl bonds as well and, in every case, the relative order of $C-Cl_{eq}/C-Cl_{ax}$ bonds follows the same pattern. For example, one can observe an analogue of the reverse Perlin effect in compounds **11**−**13** and **14b** and an analogue of the normal Perlin effect due to the elongation of the axial C−Cl bond in 3,3-dichloropiperidine **14a** which compensates for the larger magnitude of the W-effect.

Accentuation of Homoanomeric Interactions by Stretching of Acceptor Bonds. The relatively small homoanomeric interactions in the model compounds discussed above are amplified dramatically when acceptor bonds are further stretched and polarized such, as for example in the process of heterolytic bond cleavage. We will start this section with an illustrative discussion of stretching of the equatorial β-C−Cl bond in 3-chloropiperidine where the interacting orbitals adopt the W-geometry is transformed into anchimeric assistance by nitrogen lone pair to chloride ionization. In this process, the homoanomeric interaction is smoothly transformed into a bond breaking/bond-forming event, and the line between hyperconjugation and chemical reactivity becomes blurry. Because the quantitative accuracy of the NBO analysis, which is based on a dominant resonance structure decreases in the case of delocalized species, the NBO data in this section should be only taken as a semi-qualitative guide to the dynamics of the bond breaking and bond forming.

The electronic changes were analyzed by NBO analysis at every step of a relaxed geometry scan which gradually increased the C−Cl distance from 1.835 Å to 3.5 Å. At every point of this scan, geometry was completely optimized with the only constraint being the desired value of the C−Cl distance. We monitored energies of the homoanomeric n(N) → β-σ^*(C−Cl) interactions, β-C−N distances (Figure 6), natural (NBO) charges at N and Cl atoms (Figure 7) and populations of nitrogen lone pair and antibonding C−Cl orbital (Figure 7).[67] All of these parameters convincingly demonstrate that homoconjugative assistance by nitrogen lone pair plays a central role in the heterolytic C−Cl bond cleavage. Different homoanomeric interactions may promote different pathways in unimolecular rearrangements facilitated by anchimeric assistance to the bond breaking. For example, Figure 6 shows that C−Cl bond stretching lead to significant increase in the energy of the n(N) → σ^*(C−Cl) interactions even at β-C−N distances (2.25 Å) which are well above that for C−N covalent bond formation. Plots in Figure 7 qualitatively illustrate how homohyperconjugation transfers electron density from the nitrogen lone pair to the acceptor σ^*(C−Cl) orbital, thus facilitating heterolytic C−Cl bond cleavage.

Structural Effects of Homoanomeric Interactions. Now when the factors controlling the magnitude of homoanomeric interactions have become clear, we shall proceed to a discussion of the structural effects resulting from these interactions. In general, hyperconjugative effects may be reflected in a number of parameters related to molecular structure and geometry such as in C−H bond length and bond strength, XCH angles, charges at carbon, hydrogen and heteroatom involved in the interaction, orbital populations etc (Table 4). In this section, we will

(67) Additional parameters are given in the Supporting Information.

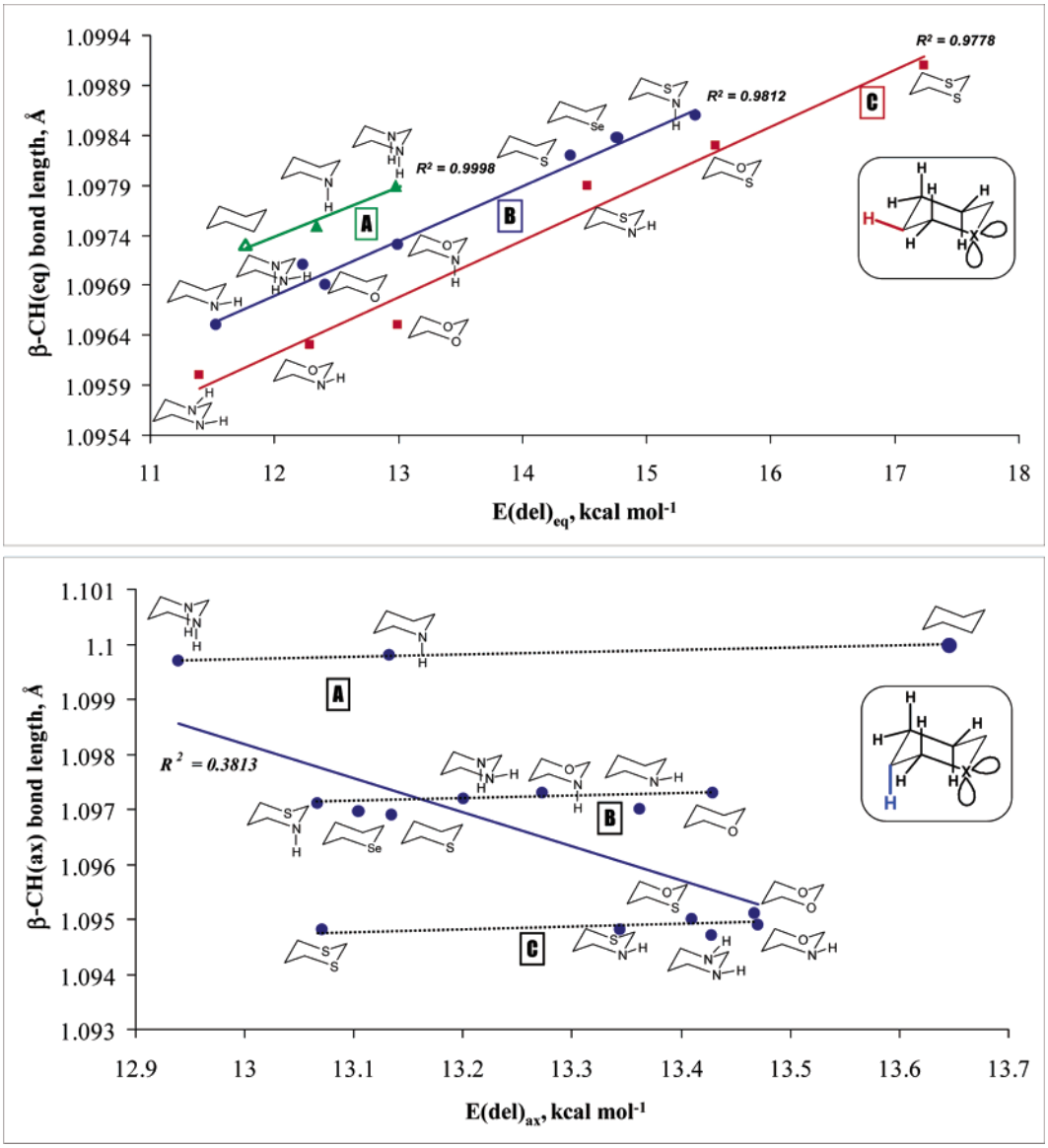

Figure 8. Contrasting correlations between NBO deletion energies for all hyperconjugative interactions (both vicinal and homoanomeric) involving axial (top) and equatorial (bottom) β-CH bonds with the respective C−H bonds lengths at the B3LYP/6-31G** level. $E(\mathrm{del})_{ax}$ and $E(\mathrm{del})_{eq}$ are defined as the sum of all homoanomeric and vicinal $\sigma\rightarrow\sigma^*$ interactions involving the respective C−H bonds: $E(\mathrm{del})_{eq} = \Sigma[n(\mathrm{X}) \rightarrow \beta\text{-}\sigma(\mathrm{C-H})_{eq}] + \sigma(\mathrm{C-C}) \rightarrow \beta\text{-}\sigma(\mathrm{C-H})_{eq} + \sigma(\mathrm{C-H}) \rightarrow \beta\text{-}\sigma(\mathrm{C-H})_{eq} + \sigma(\mathrm{C-H})_{eq} \rightarrow \sigma^*(\mathrm{C-C}) + \sigma(\mathrm{C-H})_{eq} \rightarrow \sigma^*(\mathrm{C-H})$; $E(\mathrm{del})_{ax} = \Sigma[n(\mathrm{X}) \rightarrow \beta\text{-}\sigma(\mathrm{C-H})_{ax}] + \sigma(\mathrm{C-C}) \rightarrow \beta\text{-}\sigma(\mathrm{C-H})_{ax} + \sigma(\mathrm{C-H}) \rightarrow \beta\text{-}\sigma(\mathrm{C-H})_{ax} + \sigma(\mathrm{C-H})_{ax} \rightarrow \sigma^*(\mathrm{C-C}) + \sigma(\mathrm{C-H})_{ax} \rightarrow \sigma^*(\mathrm{C-H})$.

concentrate on C−H bond length. This important structural parameter indirectly influences both C−H bond strengths (and thus reactivity) and one-bond $^1J_{C-H}$ coupling constants. Although we have previously shown that the lengths of all C−H bonds in cyclohexane, 1,3-dioxane, 1,3-dithiane, and 1,3-oxathiane correlate reasonably well with the combined energy of hyperconjugative interactions which lengthen these bonds, we have also commented that this correlation is somewhat unexpected due to the very different dipole moments, charges, populations and other factors characterizing C−H bonds in different compounds and that some of the β-C−H bond lengths were among the most deviating data in this correlation.[32] Notwithstanding these occasional deviations, one could expect such correlation, in general, to be more meaningful within a more homogeneous subset limited to C−H bonds at β-carbon atoms.

Equatorial C−H Bonds. To some extent, these expectations were met for the equatorial β-CH bonds where the magnitudes of hyperconjugative $\sigma(\mathrm{C-X}) \rightarrow \sigma^*(\mathrm{C-H})_{eq}$ and $\sigma(\mathrm{C-H})_{eq} \rightarrow \sigma^*(\mathrm{C-X})$ interactions show significant variations depending on the nature of X (11−17 kcal/mol). Figure 8 illustrates the correlation of C−H bond lengths with the combined energy of all hyperconjugative interactions elongating the respective C−H bonds (the latter value includes all vicinal as well as all homoanomeric interactions). The presence of antiperiplanar C−S bonds capable of particularly strong $\sigma(\mathrm{C-X}) \rightarrow \sigma^*(\mathrm{C-H})_{eq}$ interactions leads to the largest β-CH_{eq} bond elongation. The elongation caused by the C−O moiety is smaller than the effect of C−S bonds but still larger than the effect of C−N bonds and C−C bonds. In general, the C−H bond elongating ability of antiperiplanar C−X bonds follows the following order: C−S > C−O > C−N > C−C. Hyperconjugative donation to the σ^*(C−H) orbital seems to be particularly important as follows from the excellent correlation of the equatorial C−H bond lengths with the population of respective σ^*(C−H) orbitals (Figure 9).

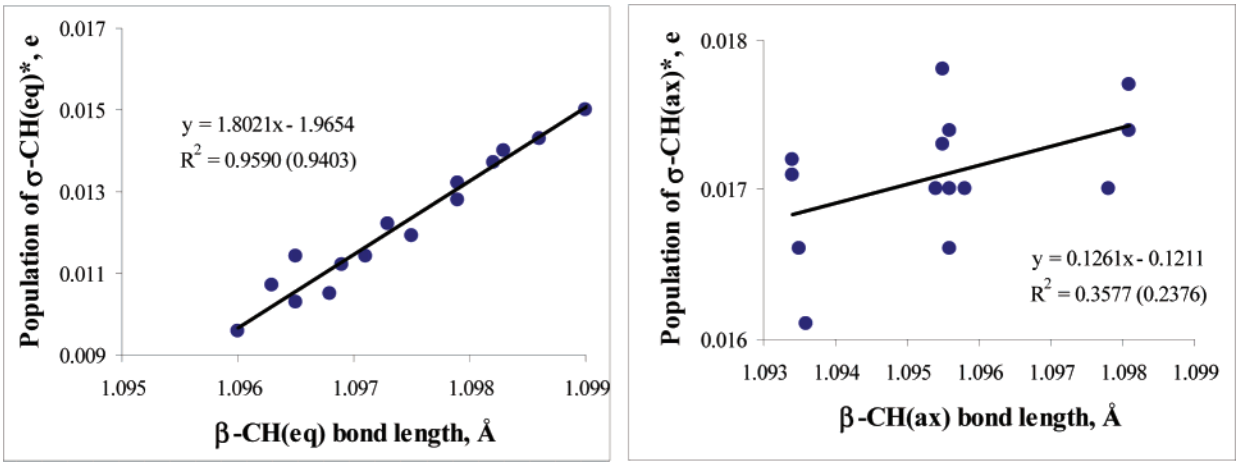

Figure 9. Contrasting correlations between population of the $\sigma^*(C-H)_{eq}$ (left) and $\sigma^*(C-H)_{ax}$ (right) orbitals with the respective C−H bond lengths computed at the B3LYP/6-31G** (B3LYP/6-311++G**) level.

Table 3. C−Cl Bond Lengths (Å) and NBO Analysis of 3,3-Dichloroheterocycles: Energies for the Dominant $n(X) \rightarrow \beta\text{-}\sigma^*(CCl)_{eq}$ Interaction (in kcal mol^{-1}) Where $n(X)$ Is $n(O)_{ax}$, $n(S)_{ax}$, $n(Se)_{ax}$, $n(N)_{eq}$, and $n(N)_{ax}$, NBO Charges on Axial and Equatorial Cl Atoms (electrons), Populations of Axial and Equatorial Lone Pairs at Heteroatoms X, $\sigma^*(C-Cl)_{eq}$ and $\sigma^*(C-Cl)_{ax}$ Orbitals (electrons), at the B3LYP/6-31G** (normal font) and B3LYP/6-311++G** (*italics*) Levels. Longer C−Cl Bonds Are Highlighted in Blue

Structure	C-Cl$_{eq}$	C-Cl$_{ax}$	E[n(N) → σ*(CCl$_{eq}$)][a]	$q_{Cl(eq)}$	$q_{Cl(ax)}$	pop σ*(CCl$_{eq}$)	pop σ*(CCl$_{ax}$)
 **11**	1.8203 *1.8196*	1.8186 *1.8180*	1.41 *1.38*	-0.029 *-0.018*	-0.028 *-0.017*	0.0723 *0.0768*	0.0749 *0.0830*
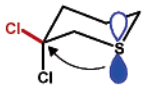 **12**	1.8358 *1.8353*	1.8169 *1.8166*	1.13 *1.23*	-0.039 *-0.028*	-0.020 *-0.013*	0.0810 *0.0890*	0.0724 *0.0815*
 **13**	1.8409 *1.8415*	1.8177 *1.8176*	1.14 *0.98*	-0.044 *-0.032*	-0.021 *-0.013*	0.0860 *0.0930*	0.0722 *0.0815*
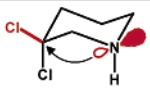 **14a**[b]	1.8222 *1.8218*	1.8318 *1.8309*	1.46 *1.35*	-0.034 *-0.024*	-0.054 *-0.044*	0.0744 *0.0798*	0.0800 *0.0887*
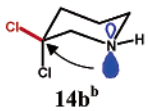 **14b**[b]	1.8250 *1.8243*	1.8188 *1.8186*	0.58 *0.70*	-0.037 *-0.025*	-0.028 *-0.018*	0.0692 *0.0746*	0.0746 *0.0836*

[a] The second-order perturbation energies for the interaction of heteroatom lone pairs (axial lone pair of O, S and Se, and equatorial/axial lone pair of N) with β-C−Cl equatorial bond (energies of other homoanomeric interactions are in the range 0.05−0.12 kcal/mol and not given in this table). [b] The isomer **14a** is more stable than **14b** by 2.6 kcal mol^{-1}.

Nevertheless, a closer scrutiny reveals that the results are not homogeneous but rather cluster in three different groups (Figure 8). Structures belonging to these three groups can be distinguished by the following criteria: (a) the combined number of β-CH_2 groups and β-equatorial nitrogen lone pairs is equal to *two*; (b) at *least one* CH_2 group *or* equatorial nitrogen lone pair is at the β-position; and (c) *neither* β-CH_2 groups *nor* β-nitrogen equatorial lone pairs are present in the molecule.

Axial C−H Bonds. Interestingly, the results for the respective axial C−H bonds cluster into the same three groups, even though a correlation with the combined energy of hyperconjugative interactions is essentially absent, and the overall situation is more complicated. The magnitudes of hyperconjugative interactions are almost the same for all C−H axial bonds,[68] and if hyperconjugation were controlling, one could have expected very small variations in the respective C−H bond lengths. However, the variations are much larger for axial than for equatorial C−H bonds; in fact, the difference in the axial β-CH bond lengths is 50% larger than that between the shortest and the longest equatorial β-CH bonds. Interestingly, although the data for the axial C−H bonds cluster into the same three groups as for their equatorial counterparts, transition from one group to another results in a 5-fold larger (ca. 0.025 Å) C−H bond elongation than in the case of equatorial C−H bonds. It is

(68) This is expected because the dominant vicinal $\sigma(C-H) \rightarrow \sigma^*(C-H')$ interactions are almost the same for these compounds.

Table 4. NBO Analysis of the Homoanomeric Interactions in the Saturated Heterocycles: Interaction Energy ($n \rightarrow \sigma^*$) between the Axial Chalcogenes (O, S, and Se) Lone Pair and β-CH_{eq} Bond (kcal mol^{-1}), Charges on Both H_{eq} and H_{ax} at the β-Carbon Atom, Population $\sigma^*(CH)_{eq}$ and $\sigma^*(CH)_{ax}$ Orbitals (e) Computed at the B3LYP/6-31G** Level (B3LYP/6-311++G** data are in *italics*)

Structure	E[n(N)→σ*(CH_{eq})]	$q_{H(eq)}$	$q_{H(ax)}$	pop σ*(CH_{eq})	pop σ*(CH_{ax})
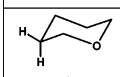 **1**	0.56 *0.61*	0.242 *0.201*	0.236 *0.195*	0.0112 *0.0120*	0.0152 *0.0170*
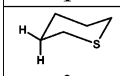 **2**	0.60 *0.68*	0.243 *0.200*	0.241 *0.198*	0.0137 *0.0161*	0.0151 *0.0173*
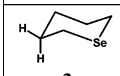 **3**	0.62 *0.72*	0.243 *0.201*	0.242 *0.200*	0.0150 *0.0172*	0.0153 *0.0178*
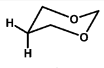 **4**	0.57 *0.62*	0.245 *0.206*	0.246 *0.206*	0.0114 *0.0112*	0.0147 *0.0161*
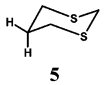 **5**	0.58 *0.69*	0.248 *0.204*	0.254 *0.210*	0.0156 *0.0185*	0.0150 *0.0172*
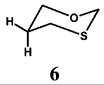 **6**	0.57 (O); 0.62 (S) *0.61*(O); *0.73*(S)	0.247 *0.206*	0.251 *0.209*	0.0140 *0.0156*	0.0148 *0.0166*

[a] The second-order perturbation energies (the energies of other homoanomeric interactions are in the range 0.05−0.12 kcal/mol, see also the deletion energies in Table 8).

obvious from Figure 8 that the effect causing this bond elongation *is not hyperconjugation*. This notion is also consistent with the poor correlation of the axial C−H bond length with the population of respective σ^*(C−H) orbitals (Figure 9), an observation which contrasts dramatically with the excellent correlation which exists for the respective equatorial C−H bonds. Although *within* every group the small changes in the energy of delocalizing interactions do seem to correlate (albeit marginally) with the almost negligible changes in the bond lengths, hyperconjugation cannot explain the sudden C−H bond elongation when one goes *from one group to another*. A different effect has to be responsible for the observed differences in the axial C−H bond lengths.

An insight into the reason for the bond elongation comes from the observation that, instead of E(del) and population of σ^*(C−H), the observed axial β-C−H bond lengths correlate well with the charge at the respective hydrogen atom (Figure 10). This observation indicates that the elongation of the axial C−H bonds and the intramolecular redistribution of electron density which decreases the positive charge at the hydrogen at the β-position may be related. Although there is no stabilizing hyperconjugative $n(N)_{eq} \rightarrow \sigma^*(CH)_{ax}$ interaction associated with this electron density transfer (Figure 8, Figure 9) due to the unfavorable topology for this interaction where the donor orbital points to the node of the acceptor orbital,[69] the repulsive four-electron (exchange) interaction between the occupied $n(N)_{eq}$ and σ_{ax} orbitals may be significant and contribute to the change in polarization of the axial C−H bonds.

"The C−H bond lengthening effect" of a β-CH_2 group and the observation that an equatorial nitrogen lone pair mimics the effect of a CH_2 group so closely are also surprising. To the best of our knowledge, these effects have not been reported and analyzed previously. This observation may warrant a separate study but we believe that it can be traced to changes in hybridization caused by the presence of a heteroatom at the β-position. In short, the β-carbon atom in heterocyclohexanes has to use a hybrid orbital with more p-character to form the C−C bond with the α-carbon atom. This is a result of α-C−X bond polarization and a direct consequence of Bent's rule for X = O and N.[70] Polarization effects propagate through bonds and lead to increased p-character (decreased s-character) in the C_α−C_β bond forming hybrid at C_β (in other words, the α-C atom becomes more electronegative than the β-C atom). Because the total s- and p-characters at every carbon atom are conserved, this decrease in s-character leads to an automatic increase in the total s-character in other hybrid orbitals at C_β including the two C_β−H bonds (Table 5). This increase is larger for the axial C−H bonds, which may lead to their shortening compared to the axial C−H bonds in cyclohexane.[71] This effect will be important for the discussion of experimental data in one of the following sections.

Thus, the general picture describing the relative trends in β-CH bond length are as follows. For equatorial C−H bonds, hyperconjugation is a controlling factor. For axial bonds, hyperconjugation is of secondary importance and the relative bond lengths are determined by intramolecular electron transfer through exchange interactions and polarization-induced rehybridization of σ-bonds.

Effect of Homoanomeric Interactions on Conformational Equilibrium. The relative stabilities of axial and equatorial azacyclohexanes in Table 6 are controlled by two factors − by differences in the acceptor ability of σ^*(C−H), σ^*(C−C), and σ^*(C−X) orbitals and by homoanomeric interactions. Interestingly, there are cases when the energies of $n(N)_{eq} \rightarrow$ α-σ^*(C−C) and $n(N)_{ax} \rightarrow$ α-$\sigma^*(C-H)_{ax}$ interactions in **7a** and **7b** are very close (7.5 and 7.7 kcal/mol respectively) and homoanomeric interactions become a dominant factor in controlling the conformational equilibrium (see Table S4 in the Supporting Information). In fact, the larger stability of the axial conformer **7a** can be ascribed to the larger magnitude of the W-effect compared with the magnitude of the $n(N)_{ax} \rightarrow \beta$-$\sigma^*$(C−H) interaction in **7b** ($\Delta E = 2x(0.6-0.3) = 0.6$ kcal/mol of extra homoanomeric stabilization). This preference is further enhanced in compounds **14a** and **14b** due to the even larger magnitude of $n(N) \rightarrow \sigma^*$ interactions in the case of a stronger acceptor such as the C−Cl bond. We believe that these systems provide the first examples of conformational equilibrium where the relative energies of two conformers are directly controlled by a homoanomeric interaction.

The increased preference for these conformers of compounds **8**−**10** which possess an equatorial lone pairs is also a consequence of a stereoelectronic effect. Introduction of the second heteroatom X (X = N, O, S) at the β'-position substitutes C−C bonds to C−X bonds in the $n(N)_{eq} \rightarrow \sigma^*$(C−X) interactions. Because C−N, C−O, and C−S bonds are better σ-acceptors

(69) This is also consistent with the observation that the F_{ij} element for the corresponding interaction are much smaller than for $n(N)_{ax} \rightarrow \sigma^*(CH)_{ax}$ interaction in Figure 4, even though the orbital overlaps are very close in both cases.

(70) The situation for the elements from the lower periods is more complicated and exact reasons for this behavior have to be analyzed in a separate study. The differences in electronegativity seem to be less important than the effects of orbital size mismatch between C and S (Se).

(71) The same effect can explain the anomalously short $C2H_{eq}$ bond length in 1,3-dioxane.

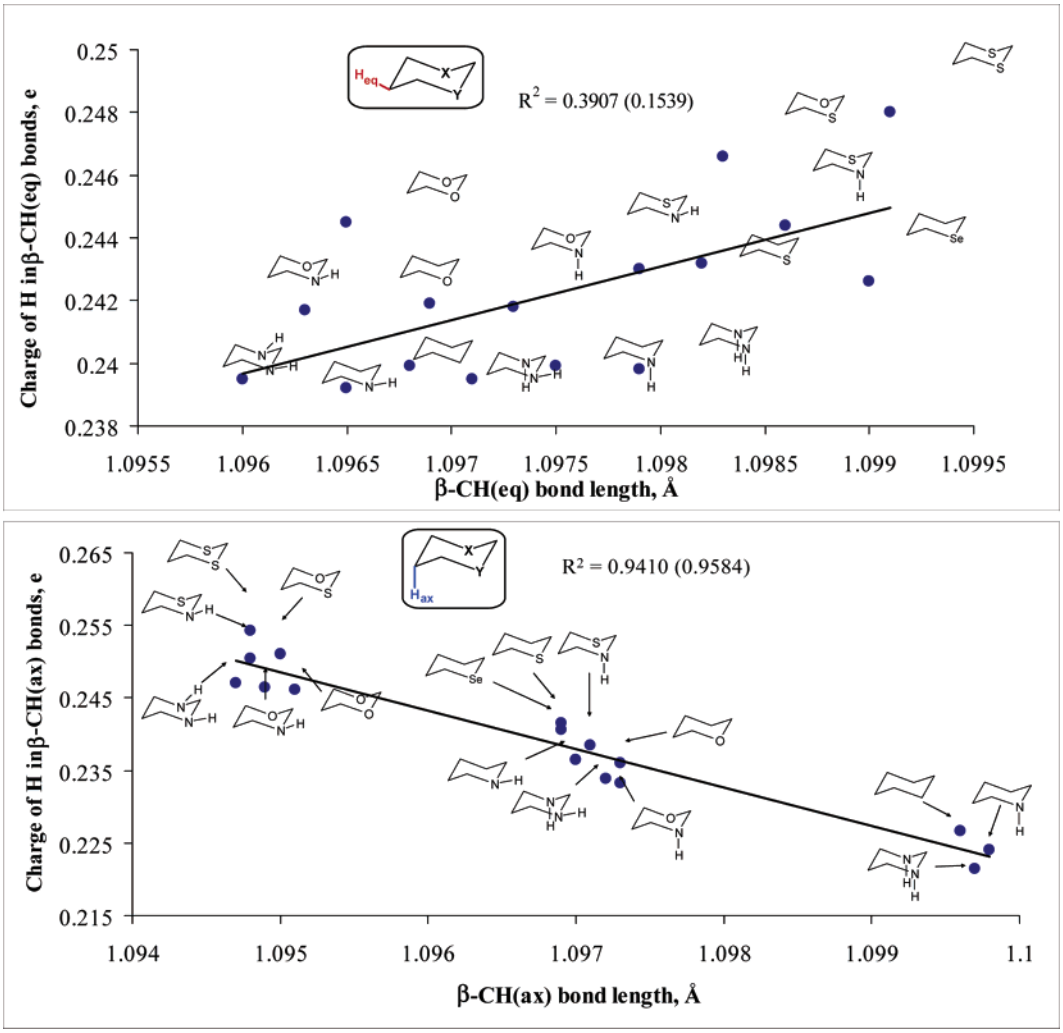

Figure 10. Contrasting correlations between NBO charges at equatorial (top) and axial (bottom) hydrogen atoms in β-CH_2 groups with the respective C−H bond lengths at the B3LYP/6-31G** (B3LYP/6-311++G**) level.

Table 5. Changes in the Hybridization (s-character percentage and sp^n notation) in the X1−C2−C3 Moiety Due to the Presence of Heteroatoms X (calculated at the B3LYP/6-31G** Level)

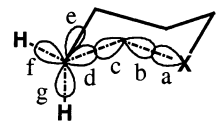	X = CH_2	X = NH_{ax}	X = NH_{eq}	X = O	X = S	X = Se
A	26.91 ($sp^{2.71}$)	29.94 ($sp^{2.34}$)	29.66 ($sp^{2.37}$)	27.89 ($sp^{2.58}$)	15.18 ($sp^{5.55}$)	11.47 ($sp^{7.47}$)
B	26.91 ($sp^{2.71}$)	23.51 ($sp^{3.25}$)	23.62 ($sp^{3.23}$)	20.53 ($sp^{3.86}$)	20.54 ($sp^{3.86}$)	18.51 ($sp^{4.40}$)
C	26.91 ($sp^{2.71}$)	28.63 ($sp^{2.49}$)	27.88 ($sp^{2.59}$)	29.42 ($sp^{2.40}$)	29.78 ($sp^{2.36}$)	30.40 ($sp^{2.29}$)
D	26.91 ($sp^{2.71}$)	26.65 ($sp^{2.75}$)	26.42 ($sp^{2.78}$)	26.21 ($sp^{2.81}$)	26.40 ($sp^{2.78}$)	26.68 ($sp^{2.75}$)
E	26.91 ($sp^{2.71}$)	26.89 ($sp^{2.72}$)	26.84 ($sp^{2.72}$)	26.87 ($sp^{2.72}$)	27.10 ($sp^{2.69}$)	27.13 ($sp^{2.69}$)
F	23.55 ($sp^{3.24}$)	23.77 ($sp^{3.20}$)	23.60 ($sp^{3.23}$)	23.77 ($sp^{3.20}$)	23.32 ($sp^{3.28}$)	23.22 ($sp^{3.30}$)
G	**22.58 ($sp^{3.43}$)**	**22.65 ($sp^{3.41}$)**	23.10 ($sp^{3.33}$)	23.11 ($sp^{3.32}$)	23.10 ($sp^{3.33}$)	23.01 ($sp^{3.34}$)

than C−C bonds,[59] $n(N)_{eq} \rightarrow \sigma^*(C-X)$ interactions are stronger than $n(N)_{eq} \rightarrow \sigma^*(C-C)$ interactions and conformers of azacyclohexanes **8**−**10** with equatorial lone pairs are significantly more stable than their counterparts with axial lone pairs. For example, the energies for the corresponding $n(N)_{eq} \rightarrow \sigma^*(C-X)$ interactions (in kcal/mol) were found to be equal 7.5 for X = C; 10.6 for X = N−H_{eq}; 9.5 for X = N−H_{eq} (see the Supporting Information section for more details).[72]

(72) For other effects of analogous of $n(N) \rightarrow \sigma^*(C-N)$ interactions, see: Hetényi, A.; Martinek, T. A. Lázár, L.; Zalán, Z.; Fülöp, F. *J. Org. Chem.* **2003**, *68*, 5705. See also: Neuvonen, K, Fülöp, F.; Neuvonen, H.; Koch, A.; Kleinpeter, E.; Pihlaja, K. *J. Org. Chem.* **2001**, *66*, 4132.

Table 6. Relative Energy (kcal mol^{-1}) of Different Conformers and NBO Analysis of the Homoanomeric Interactions in the Saturated Heterocycles: Interaction Energy ($n \rightarrow \sigma^*$) between the Axial (O, S, Se, and N) and Equatorial (N) Heteroatom Lone Pair and β-CH_{eq} Bond (kcal mol^{-1}), Charges on Both H_{eq} and H_{ax} at the β-Carbon Atom and Population of X Lone Pairs and $\sigma^*(CH)_{eq}$ as well as $\sigma^*(CH)_{ax}$ Orbitals (e) Computed at the B3LYP/6-31G** Level (B3LYP/6-311++G** data are in *italics*)

Structure	ΔE (ax/eq)	E[n(X)→ σ*(CH_{eq})][a]	$q_{H(eq)}$	$q_{H(ax)}$	pop σ*(C-H_{eq})	Pop σ*(C-H_{ax})
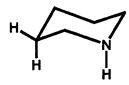 **7a**	0.0 *0.0*	0.56 *0.62*	0.240 *0.198*	0.224 *0.186*	0.0119 *0.0129*	0.0154 *0.0174*
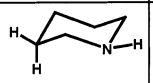 **7b**	0.3 *0.7*	0.26 *0.29*	0.239 *0.197*	0.237 *0.195*	0.0103 *0.0113*	0.0155 *0.0174*
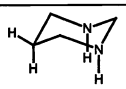 **8a**	0.0 *0.0*	0.57[b] *0.64*	0.240 *0.200*	0.222 *0.183*	0.0128 *0.0132*	0.0154 *0.0170*
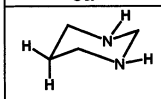 **8b**	3.6 *2.6*	0.23[b] *0.25*	0.240 *0.199*	0.247 *0.206*	0.0096 *0.0101*	0.0154 *0.0171*
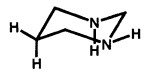 **8c**	0.4 *0.1*	0.53 (0.25)[b] *0.59 (0.28)*	0.234 *0.194*	0.240 *0.199*	0.0114 *0.0118*	0.0153 *0.0170*
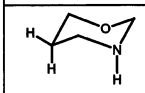 **9a**	0.0 *0.0*	0.58(O); 0.56(N) *0.63(O); 0.64(N)*	0.242 *0.203*	0.233 *0.194*	0.0122 *0.0123*	0.0151 *0.0166*
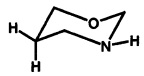 **9b**	3.6 *3.2*	0.54(O); 0.26(N) *0.57(O); 0.29(N)*	0.242 *0.202*	0.246 *0.206*	0.0107 *0.0107*	0.0150 *0.0166*
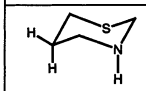 **10a**	0.0 *0.0*	0.54(S); 0.63(N) *0.61(S); 0.72(N)*	0.244 *0.203*	0.238 *0.197*	0.0143 *0.0161*	0.0151 *0.0170*
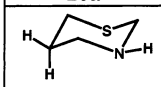 **10b**	3.6 *3.1*	0.59(S); 0.25 (N) *0.68(S); 0.29(N)*	0.243 *0.201*	0.251 *0.208*	0.0132 *0.0150*	0.0152 *0.0172*

[a] The second-order perturbation energies for the interaction and the energies of other homoanomeric interactions are in the range 0.04−0.11 kcal/mol (see Table 4). [b] Only single value is considered for **8a** and **8b** due to symmetrical N lone pairs whereas two values for unsymmetrical N lone pairs in **8c** are in the format axial (equatorial).

Role of Geometry and Structural Constraints. To investigate the role of molecular geometry and orbital overlap further, we compared model compounds **15b** and **32**−**34** all of which have a nitrogen atom at the β-position relative to a C−Cl bond (Figure 11). In every case, a homoanomeric $n(N)_{eq} \rightarrow \sigma^*(C-Cl)_{eq}$ interaction is possible and, indeed, present. However, different degrees of molecular constraints and internal rigidity change the energies of these interactions. In the first case, an acyclic molecule, both nitrogen and C−Cl bonds are not bound by any constraints. In the second case, the C−Cl bond is exocyclic and capable of adjusting its orientation to maximize the stabilizing stereoelectronic interaction. In the third case, although the orientation of both donor and acceptor orbitals is fixed by the cyclic structure, the ring is relatively flexible. In the fourth case, the bicyclic structure imposes the most unfavorable geometric restraints on the interaction—not only is the distance rather large but also the lone pair orientation is less favorable for interaction with the σ^*(C−Cl) orbital.

The differences in the magnitude of $n(N) \rightarrow \sigma^*(C-Cl)$ interactions in the first three compounds of Figure 11 are not large. It is interesting that relaxing the restraints does not increase the interaction energy in a uniform way. This is not surprising because there are other stereoelectronic requirements which have to be satisfied (for example antiperiplanar placement of vicinal donor and acceptor orbitals) in addition to maximizing the $n(N) \rightarrow \sigma^*(C-Cl)$ interaction. However, the most instructive effect is the 50% drop in energy of the W-interaction in bicyclic diamine **34** which is closely structurally related to the diamine used in the mechanistic study aimed at proving the existence of the W-effect (discussed in the next section).[35] This result stresses the necessity for exercising extreme caution when transferring stereoelectronic interactions from one molecule to

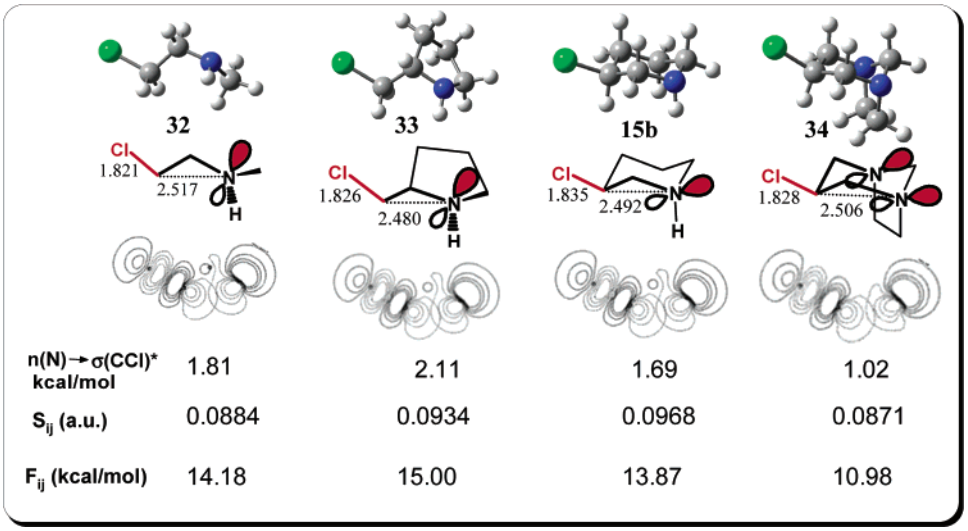

Figure 11. Effect of cyclic restraints on n(N)→σ*(C−Cl) homohyperconjugation.

another, even when these molecules are close in structure. Theory plays a pivotal role here in placing stereoelectronic arguments on solid ground and should be used for supporting and rigorous testing of these arguments whenever they are claimed to be important.

Analysis of Experimental Studies of Homoanomeric Interactions in 1,3-Diazacyclohexanes. The above analysis helps us for an understanding of the stereoelectronic interactions in a series of substituted 1,3-diazacyclohexanes studied by Anderson, Davies, and co-workers (Table 7).[35] This elegantly designed experimental study intended to elucidate the relative importance of the two homonoanomeric effects—the $n(X)_{ax} \rightarrow \sigma^*(C-Y)_{eq}$ and $n(X)_{eq} \rightarrow \sigma^*(C-Y)_{eq}$ interactions—in nitrogen containing heterocycles by restraining the nitrogen lone pairs to either an axial or an equatorial position. For 1,3-di-*tert*-butyl-1,3-diazacyclohexanes where the bulky *tert*-Bu groups are oriented equatorially and the nitrogen lone pairs oriented axially, the main homoanomeric interaction should be that of the axial nitrogen lone pairs with the equatorial C−H bonds on the β-methylene group (the Plough effect). On the other hand, the unshared electron pairs are oriented equatorially in 1,5-diazabicyclo[3.2.1]octanes and, thus, should be capable of participating in the W-plan $n_{eq} \rightarrow \sigma^*_{C-H}$ interaction.

However, despite the elegant experimental design, this work could not arrive at a definitive conclusion about the importance of two possible homoanomeric effects due to several reasons. The first complication resulted from the difficulties in unambiguously assigning of the coupling constants. In several cases, it was not possible to separate one-bond coupling constants of similar size, especially at low temperatures where additional line broadening was present. For example, the C5−H coupling constants for di-*tert*-butyl-1,3-diazacyclohexane were determined as an average for the axial and the equatorial values (127.4 Hz) and the coupling constants for the 1,5-diazabicyclo[3.2.1]octane were not determined.

The other limitation was the lack of information about the respective C−H bond lengths, which made some of the spectral assignments quite risky. For example, the coupling constants for 8-methyl-1,5-diazabicyclo[3.2.1]octane (measured as 125.2 and 127.4 Hz) were assigned tentatively to the axial and equatorial C−H couplings, respectively. This assignment was based on the assumption that the axial $^1J_{C3H}$ couplings in 8-methyl-1,5-diazabicyclo[3.2.1]octane and 3,8-dimethyl-1,5-diazabicyclo[3.2.1]octane are the same or similar. However, a comparison of the calculated C−H bond lengths in these two

Table 7. Comparison of C−H Bond Lengths at the β-Carbons of Two Conformers of 1,3-Diazacyclohexane and Their Derivatives Studied Experimentally (ref 35) along with the Energies of n(N) → $\sigma^*(C-Y)_{eq}$ (E_1) and n(N) → $\sigma^*(C-Y)_{ax}$ (E_2) Homoanomeric Interactions (kcal mol^{-1}) and s-character (%) in the Carbon Hybrid Orbitals Forming the β-CH_{eq} and β-CH_{ax} Bonds (B3LYP/6-31G** computations)

Compound	E_1	E_2	s-char $C(H_{eq})$	s-char $C(H_{ax})$
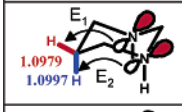	1.36	0.00	24.01	22.77
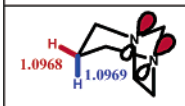	0.71	0.00	24.11	22.99
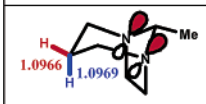	0.59	0.00	24.10	22.98
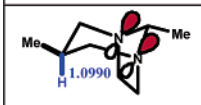	N/A	0.00	N/A	21.97
	0.67	0.05	23.48	22.59
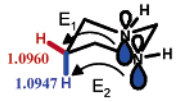	0.55	0.24	23.66	23.65
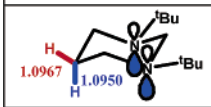	0.63	0.21	23.39	23.38
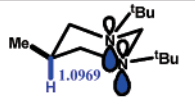	N/A	0.20	N/A	22.41

compounds shows that this assumption is not warranted. The C−H bond lengths in the 3-Me-substituted diazabicyclo[3.2.1]-octane is significantly longer due to the hyperconjugative $\sigma_{C-H} \rightarrow \sigma^*_{C-H}$ of the axial C−H bond with the C−H bonds from the methyl group. Most likely these assignments should be reversed with the axial coupling in 8-methyl-1,5-diazabicyclo-[3.2.1]octane smaller than the equatorial coupling: the axial C−H bond is slightly longer and, more importantly, it has less s-character (Table 7) which should decrease the contribution of the Fermi contact to the coupling constant. Note, also that in 2,2,4,8-tetramethyl-1,5-diazabicyclo[3.2.1]octane the axial and equatorial $^1J_{CH}$ were found to be "not detectably different" with a value of 125 Hz which is likely to be a result of the experimental difficulties discussed above.

In addition, the geometric restraints in the two sets of the model compounds in Table 7 considerably change the magnitudes of the stereoelectronic effects they intended to illustrate. The W-effect in diazabicyclo[3.1.1]nonane is only about half of the usual magnitude of this effect in the less constrained azacyclohexanes. On the other hand, the unusually high p-character of *tert*-Bu-substituted nitrogen lone pairs increases the magnitude of $n(N)_{ax} \rightarrow \sigma^*(C-H)_{eq}$ interaction. Combination of these effects makes these two hyperconjugative interactions very similar in magnitude in the above model compounds. As a result, the relative bond lengths inside of the CH_2 pairs is controlled by the unusual bond-elongating effect of equatorial N lone pairs which leads to the additional elongation of the axial β-C−H bonds in diazabicyclo[3.1.1]nonanes. The W-effect in diazabicyclo[3.1.1]nonane is of secondary importance in determining the difference between the axial and equatorial β-CH bond lengths.

This result also illustrates that one should be careful in using differences in the axial and the equatorial C−H bond lengths *within a given molecule* as proof for the existence of homoanomeric interaction—either the W-effect or the Plough effect. In azacyclohexanes with an axial lone pair, the equatorial β-C−H bond in the β-CH_2 group is longer whereas in azacyclohexanes with an equatorial lone pair the axial β-C−H bond is longer. However, the superficial conclusion that the Plough effect is larger than the W-effect in these molecules would be incorrect. If one compares the *equatorial* bond lengths *between* the two conformers of 1,3-diazacyclohexane, then it is clear that the W-effect in one conformer leads to a larger β-C−H_{eq} bond elongation than the Plough effect in the other conformer.

Cooperativity of the Hyperconjugative Interactions. Although this is a rather technical part of this paper, it reports practically important general trends which are also theoretically intriguing. Although the dissection of homoanomeric contributions from each lone pair is theoretically may be instructive, from a practical point of view one is more likely to be concerned with the combined effect of two oxygen lone pairs. This brings up an interesting question whether the hyperconjugative energies with participation of different orbitals are additive.[73] In other words, one can ask whether the simultaneous deletion of two interactions from the Fock matrix will give the same result as the arithmetic sum of the two deletions corresponding to the individual interactions. For example, it is not clear whether the energy of $n(O)_{ax} \rightarrow \sigma^*(C-Y) + n(O)_{eq} \rightarrow \sigma^*(C-Y)$ NBO deletions is equal to the energy of the $(n(O_{ax+eq}) \rightarrow \sigma^*(C-Y))$ combined NBO deletion. Because NBO deletion analysis is a variational procedure, the energy price for the simultaneous loss (deletion) of two hyperconjugative interactions is not equal to the sum of the individual NBO deletion energies for these two interactions. Thus, NBO analysis is highly appropriate for studies of cooperativity effects in orbital interactions which reflect symmetry of the wave function. When the energy of the simultaneous deletion of two interactions from the Fock matrix is less than the sum of two individual interactions, we will call this pattern "anticooperative". When it is larger, we will call this pattern "cooperative". If there is no difference, the interactions are purely additive.[74]

To the first approximation, all homoanomeric interactions from one heteroatom donor to one σ^*-acceptor [(a + c) and (b + d) in Table 8 and Tables S8−S9 in the Supporting Information section] are additive and, thus, we can compare total donating abilities of different heteroatoms by simply comparing the sums of donating abilities of their lone pairs. Such a comparison is important for practical reasons because the summation of effects from two lone pairs eliminates any potential ambiguity that may be present (or perceived to be present) due to different theoretical models for the lone pairs and or due to different approaches to orbital localization. Because the donation to the β-σ^*_{C-H} orbitals is additive, we can conclude that the order of donor ability of heteroatoms in homoanomeric interactions is O < S < Se but the differences in the interaction energies are hardly important at the energy minimum conformations.

By contrast, some of the other hyperconjugative patterns are not simply additive.[75] These deviations from additivity are small but reproducible at different levels of theory and for different heteroatoms. For example, donation from a lone pair to two σ^*_{C-H} orbitals is cooperative whereas donation from two lone pairs to the same σ^*_{C-H} orbital is anticooperative (Figure 12).[76] At first glance, the second effect seems to be perfectly consistent with chemical intuition: one can argue that donation from one lone pair increases electron density at the acceptor orbital and decreases its acceptor ability toward the second lone pair. However, the constructive interference of two $n \rightarrow \sigma^*(C-H)/\sigma^*(C-H')$ interactions is counterintuitive and is not consistent with the above logic. Why is donation from a lone pair to two acceptors better than donation to a one acceptor? Instead, one could expect that transfer of the electron density from a lone pair to an acceptor decreases the donor ability of this lone pair toward the second acceptor. However, in reality the situation is just the opposite and this is a reflection of the wave function symmetry and some of the most general rules of structural organic chemistry.

(73) An interesting effect of "colliding" anomeric interactions was discussed in Cramer, C.; Kelterer, A. -M., French, A. D. *J. Comp. Chem.* **2001**, *22*, 1194. Cooperativity in the effects of anomeric interactions on the C−H bond length and one-bond $^1J_{C-H}$ coupling constants was analyzed recently (Cuevas, G.; Juaristi, E. *J. Am. Chem. Soc.* **2002**, *124*, 13 088) but cooperativity in energies of such interactions has not been studied so far.

(74) This follows a convention suggested in ref 16. Several fascinating examples of cooperative and anticooperative hyperconjugative arrays are given in "Valency and Bonding: A Natural Bond Orbital Donor−Acceptor Perspective". Weinhold, F.; Landis, C. R. Cambridge Press (in press) and in ref 2.

(75) After this paper has been submitted, a thorough NBO analysis of cooperativity effects in hydrogen bonding of base pairs appeared in the literature: Sproviero, E. M.; Burton, G. *J. Phys. Chem. A* **2003**, *107*, 5544.

(76) There are other small but reproducible differences: $(a + c) + (b + d)$ is always less or equal to $(a + b + c + d)$ whereas $(a + b) + (c + d)$ is always equal or larger than $(a + b + c + d)$.

Table 8. NBO Deletion Energies (kcal mol^{-1}) and Cooperativity Effects for the Homoanomeric Interactions in the Saturated Heterocycles ($n\rightarrow\sigma^*$) Calculated at the B3LYP/6-31G** Level

Structure	$n(X)_{eq}\rightarrow\sigma^*(CH_{eq})$ **(a)**	$n(X)_{eq}\rightarrow\sigma^*(CH_{ax})$ **(b)**	$n(X)_{ax}\rightarrow\sigma^*(CH_{eq})$ **(c)**	$n(X)_{ax}\rightarrow\sigma^*(CH_{ax})$ **(d)**	**(a+c)**	**(b+d)**	**(a+b)**	**(c+d)**	**(a+b + c+d)**
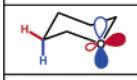	0.05	0.11	0.66	0.00	0.71	0.11	0.16	0.66	0.83
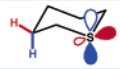	0.01	0.10	0.74	0.12	0.75	0.22	0.11	0.87	0.98
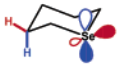	0.00	0.09	0.78	0.15	0.78	0.25	0.09	0.95	1.05
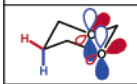	0.02[a] 0.05[b]	0.08 0.17	0.67 1.29	0.00 0.00	0.69 1.33	0.09 0.17	0.11 0.21	0.67 1.31	0.78 1.50
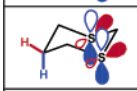	0.00 0.00	0.15 0.30	0.72 1.40	0.09 0.17	0.72 1.40	0.25 0.49	0.15 0.30	0.81 1.60	0.98 1.91
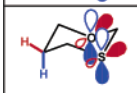	0.01[c] 0.00[d] 0.01[e]	0.13 0.09 0.22	0.66 0.77 1.39	0.00 0.11 0.11	0.66 0.77 1.39	0.13 0.20 0.33	0.14 0.09 0.23	0.66 0.89 1.51	0.80 0.98 1.74

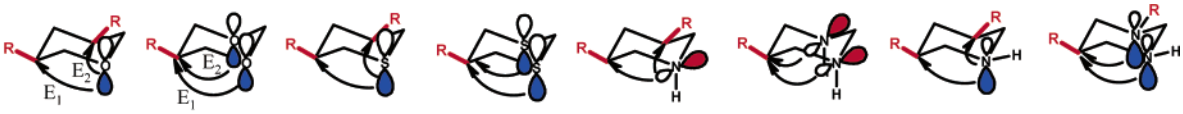

$E_1=E_2$:	0.655	0.660	0.741	0.722	0.703	0.708	0.317	0.278
R = H E_{tot} :	1.382	1.294	1.565	1.403	1.496	1.360	0.672	0.546
ΔE :	**0.072**	***-0.036***	**0.083**	***-0.041***	**0.090**	**-0.056**	**0.038**	**-0.010**
$E_1=E_2$:	1.582	1.424	1.605	1.342	1.710	1.611	0.889	0.620
R = Cl E_{tot} :	3.436	2.742	3.486	2.589	3.781	3.054	1.914	1.210
ΔE :	**0.272**	***-0.106***	**0.276**	***-0.095***	**0.361**	***-0.168***	**0.136**	***-0.030***

Figure 12. Cooperative (bold) and anti-cooperative (*bold italics*) effects on homoanomeric interactions involved in the respective mono and di-substituted heterocycles. $\Delta E = E_{tot} - (E_1 + E_2)$, where E_1 and E_2 are the energies of two possible homoanomeric interactions and E_{tot} is energy determined by combined NBO deletion.

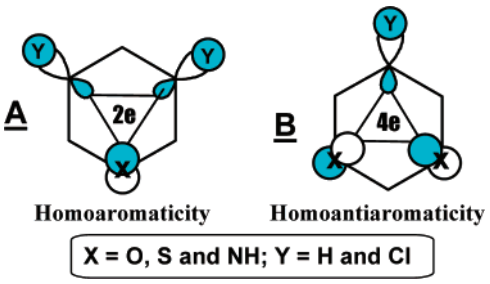

Figure 13. σ-Homoaromaticity (**A**) and antiaromaticity (**B**) in six-membered heterocycles.

The contrasting cooperativity effects can be predicted by considering the number of electrons participating in the interaction pattern. There are *two* electrons in the cyclic array of orbitals involved in the cooperative $2\sigma^* + n(X)$ interaction which satisfies the 4n+2 rule for aromaticity. By contrast, the $\sigma^* + 2n(X)$ interaction involves *four* electrons and can be considered antiaromatic according to the 4n criterion (Figure 13).

From a slightly different but intrinsically related perspective, the same prediction could also be made by inspecting the symmetry of the frontier MOs (FMOs) in these molecules. In 1,3-diheterocyclohexanes, the HOMO is an asymmetric combination of the lone pairs which cannot interact simultaneously with the σ^*(C5−Y) orbital. By contrast, the LUMO of the oxa- and azacyclohexanes is a linear combination of MOs which involves the symmetric combination of σ^*(C3−Y) and σ^*(C5−Y) orbitals with the suitable symmetry for simultaneous interaction of both σ^*-orbitals with the lone pair at X. Interestingly, when the interaction increases in magnitude 2.5 times (change from C−H to C−Cl), the cooperativity effect increases four times (Figure 12). A further increase in acceptor ability of σ^* orbital should transform the $2\sigma^* + n(X)$ interaction into the classic σ-homoaromatic array[77] and lead to other interesting phenomena[78] which we will discuss in a separate paper.

Conclusion. Homoanomeric interactions lead to noticeable changes in geometries, electronic structure, conformational

(77) Winstein, S. *J. Am. Chem. Soc.* **1959**, *81*, 6524. For recent discussions of homoaromaticity, see: Holder, A. *J. Comput. Chem.* **1993**, *14*, 251. Williams, R. V. *Chem. Rev.* **2001**, *101*, 1185. Stahl, F.; Schleyer, P. v. R.; Jiao, H.; Schaefer, H. F., III; Chen, K.-H.; Allinger, N. L. *J. Org. Chem.* **2002**, *67*, 6599. Homoaromaticity in transition states: Jian, H.; Nagelkerke, R.; Kurtz, H. A.; Williams, V.; Borden, W. T.; Schleyer, P. v. R. *J. Am. Chem. Soc.* **1997**, *119*, 5921. Homoaromaticity in carbenes and cationic intermediates: Freeman, P. K.; Dacres, J. E. *J. Org. Chem.* **2003**, *68*, 1386. Bishomoaromatic Semibullvalenes: Goren, A. C.; Hrovat, D. A.; Seefelder, M.; Quast, H.; Borden, W. T. *J. Am. Chem. Soc.* **2002**, *124*, 3469.

(78) A similar effect of symmetry-enhanced and symmetry-forbidden hyperconjugation can lead to enhancement (or cancellation) of the β-coupling in the EPR spectroscopy of cyclic β-conjugated organic radicals: D. H. Whiffen, *Mol. Phys.* **1963**, *6*, 223. It was shown that this effect is general and can be readily extended to spin-paired molecules as well. Davies, A. G. *J. Chem. Soc., Perkin Trans.* **1999**, *2*, 2461.

equilibria and reactivity of saturated heterocycles. The effects on reactivity are 2-fold. First, homoanomeric interactions can control conformational equilibria and may increase reaction rates by preorganizing substrates into a geometry suitable for the lone pair assisted intramolecular rearrangements. Second, the effects of homoanomeric interactions increase dramatically when acceptor bonds are stretched and/or polarized. In such cases, different topologies of homoanomeric interactions can lead to contrasting reactivities and modified selectivities of unimolecular rearrangements.

Although these effects are undoubtedly general, their absolute magnitudes and relative importance should be carefully reanalyzed when new geometries and new combination of donor and acceptor orbitals are considered. Geometric restraints should be introduced with caution because such restraints in cyclic molecules can either enhance or weaken such interactions. In addition, the properties of lone pairs in O- and S-heterocycles are considerably different from their N-analogues and, thus, stereoelectronic effects observed in O-heterocycles cannot be automatically extended to the N-heterocycles and vice versa. In general, because of the differences in the interaction geometries and properties of lone pairs, any attempt to generalize stereoelectronic effects by transferring observations found for one substrate to a new class of compounds is risky.[79] Such transfer of subtle stereoelectronic interactions to different substrates should always be checked by independent experimental and theoretical studies.

Only the $n(\mathrm{O/S})_{ax} \rightarrow \beta\text{-}\sigma^*(\mathrm{C-Y})_{eq}$ (the Plough) interaction is important in O- and S-containing heterocycles. By contrast, both the Plough ($n(\mathrm{N})_{ax} \rightarrow \beta\text{-}\sigma^*(\mathrm{C-Y})_{eq}$) and the W-effect ($n(\mathrm{N})_{eq} \rightarrow \beta\text{-}\sigma^*(\mathrm{C-Y})_{eq}$ operate in N-containing heterocycles. Homoanomeric effects are considerably weaker than vicinal anomeric $n(\mathrm{X})_{ax} \rightarrow \alpha\text{-}\sigma^*(\mathrm{C-Y})_{ax}$ interactions but their importance increases significantly when the acceptor ability of antibonding orbitals increases.

Although the homoanomeric interactions discussed above are undoubtedly important for reaching an understanding of structural parameters (trends in C−H bonds lengths), spectroscopic properties (NMR assignments based on C−H coupling constants), and conformational equilibria in carbo- and heterocycles, the importance of these effects on chemical reactivity is virtually unexplored. Although the magnitude of these interactions is generally small (less than 1 kcal/mol) when relatively weak acceptors such as σ^*(C−H) orbitals are involved, these interactions are additive and their magnitude increases dramatically in the case of stronger σ-acceptors.

Acknowledgment. The authors are grateful to the National Science Foundation (CHE-0316598), Donors of the American Chemical Society Petroleum Research Fund, the Center for Materials Research and Technology (MARTECH) of Florida State University for the support of this research, the 3M Company for an Untenured Faculty Award (to I. A.), and Professors F. Weinhold (UW-Madison), A. Davies, and E. Anderson (UC London) for important discussions.

Supporting Information Available: Cartesian coordinates and total energies for all optimized geometries. Correlation of β-$\mathrm{CH_{eq}}$ bond lengths and total NBO deletion energies for the respective CH bond at the B3LYP/6-31G** level. Correlations of energies of homoanomeric interactions with the corresponding overlap and Fock matrix elements. Changes in hybridization and energies of nitrogen lone pair and σ^*(C−Cl) orbital during the process of C−Cl bond stretching in 3-chloropiperidine. The energies (kcal $\mathrm{mol^{-1}}$) of hyperconjugative interactions discussed in this paper. The hybridization of C−X bonds (X = O, S, Se and N) in heterocycles. This material is available free of charge via the Internet at http://pubs.acs.org.

JA037304G

(79) The other factors which complicate such direct comparisons are difference in electronegativities and C−X bond lengths. However, these two factors are usually handled well by chemical intuition.